Adaptive Neural Network Control for Switched Stochastic Pure-Feedback Nonlinear Systems with Incomplete Measurements

Zhongfeng Li, Lidong Wang*, Hongwei Lv, and Zhongyi Wang

Abstract—**This study explores an adaptive neural network-based output-feedback tracking control strategy for switched stochastic pure-feedback nonlinear systems with incomplete state measurements. To address challenges posed by packet loss or transmission saturation, which may distort or obstruct access to state variables, a state estimator is introduced to approximate the unmeasured states. The proposed method employs neural networks to approximate unknown nonlinearities, while dynamic surface control (DSC) is utilized to mitigate complexity explosion, a common issue in traditional backstepping control design. The results demonstrate that the control approach guarantees that all signals within the closed-loop system remain semiglobally uniformly ultimately bounded (UUB) with a certain probability. Furthermore, it is shown that the system output will asymptotically approach a small neighborhood around the desired reference signal in terms of its mean quartic value. Simulation results are provided to validate the efficacy of the proposed control method.**

Index Terms—**switched stochastic pure-feedback nonlinear systems, adaptive neural network control, incomplete measurements, dynamic surface control.**

I. Introduction

SWITCHED systems are a type of hybrid system in which the overall dynamics depend on both the control inputs of individual subsystems and a discrete switching signal. The interconnection of continuous and discrete elements poses notable challenges for controller design and stability analysis[1, 2]. Despite these difficulties, switched systems find extensive use in power systems, mechanical systems, multi-agent networks, and other complex engineering fields [3, 4]. The control theory community has placed increasing emphasis on switched nonlinear systems. For instance, Ref. [5] developed a fuzzy adaptive output-feedback control method for MIMO switched nonlinear systems with unknown control directions, specifically targeting pure-feedback architectures. By leveraging adaptive backstepping and Lyapunov-based methodologies, the authors addressed key issues stemming from switching signals. Ref. [7] further investigated output tracking control for constrained nonlinear switched systems through a barrier Lyapunov function, demonstrating how diverse techniques can tackle the complexity inherent in switching dynamics.

The adaptive backstepping technique is widely recognized for its systematic approach to controlling nonlinear systems, particularly those structured in strict-feedback form. Considerable progress has been made in this arena, especially for deterministic and non-switching scenarios [8–10]. Ref. [11] proposed an adaptive neural tracking control approach for interconnected switched systems with unmodeled dynamics, while fuzzy output feedback was utilized to address the difficulties posed by switching signals [12]. In contrast, pure-feedback systems involve non-affine relationships between input and state variables, which complicates controller design even further. Nonetheless, pure-feedback controllers remain highly relevant in domains such as chemical processes, aerospace, and mechanical systems. Ref. [13] investigated adaptive output-feedback neural network control for uncertain switched nonlinear systems in pure-feedback form, whereas Ref. [14] focused on designing neural network observers for switched stochastic nonlinear pure-feedback systems under partial error constraints. Their findings confirmed hemispherical consistency of the closed-loop signals under multiple switching conditions. Similarly, Ref. [15] introduced a robust adaptive fuzzy tracking control scheme aimed at pure-feedback stochastic nonlinear systems with input constraints, achieving uniform hemispherical boundedness of all signals.

Given that many real-world systems are influenced by random disturbances, the study of switched stochastic nonlinear pure-feedback systems has received substantial attention. Ref. [16] analyzed switched stochastic nonlinear pure-feedback nonlower triangular systems and proposed an adaptive neural tracking controller. Ref. [17] addressed fuzzy adaptive tracking control for constrained nonlinear switched stochastic pure-feedback systems, illustrating that all closed-loop signals could remain semiglobally consistent and ultimately bounded.

In practical applications, physical and technical constraints in networked control systems often lead to phenomena such as packet loss, input saturation, and time delays. These issues can degrade state measurements, particularly in wireless communication scenarios, and consequently diminish controller performance. Extensive research has investigated the

Manuscript received November 3, 2024; revised February 22, 2025.

This work was supported in part by the Fundamental Research Funds for Liaoning Provincial Joint Funds Project - General Funding Program (Grant Nos. 2023-MSLH-323 and 2023-MSLH-310), the Fundamental Research Funds for Liaoning Universities (LJ212410146009) and the Foundation of Yingkou Institute of Technology under the Institutional-Level Scientific Research Initiative (Grant Nos. FDL202404 and FDL202409).

Zhongfeng Li is an associate professor at the School of Electrical Engineering, Yingkou Institute of Technology, Yingkou 115100 China.(e-mail: afeng0601@163.com).

Lidong Wang is a professor at the School of Electronic and Information Engineering, University of Science and Technology Liaoning, Anshan 114051 China.(Corresponding author, e-mail: wangld5600@163.com).

Hongwei Lv is a postgraduate student at the School of Electronic and Information Engineering, University of Science and Technology Liaoning, Anshan 114051 China.(e-mail: lv47020@163.com).

Zhongyi Wang is a postgraduate student at the School of Electronic and Information Engineering, University of Science and Technology Liaoning, Anshan 114051 China.(e-mail: wangzhongyi0213@163.com).

influence of delays and packet loss on networked systems. For example, Ref. [18] established stability results for a class of linear switching systems subject to time delays using Lyapunov-based methods. Ref. [19] extended the study to discrete-time switched time-delay systems, deriving critical insights on stability. Ref. [20] explored stability analysis and H_∞ controller synthesis for discrete-time switched systems with time delays. Furthermore, Ref. [21] presented observer-based adaptive neural control schemes for switched stochastic pure-feedback systems encountering input saturation, examining the detrimental impact of unbounded delays and data loss on system performance.

Distinguished from prior work, this paper presents three main contributions:

(1) Recognizing that packet loss and input saturation frequently occur in practical communication channels, this study focuses on controlling switched stochastic nonlinear systems under three scenarios: normal conditions, data saturation, and data loss. Two random variables are introduced to capture a stochastic combination of ideal and degraded measurements. By comparison, Ref. [22, 25] analyzed delay-dependent stability for discrete-time switched systems with time-varying delays but did not explicitly address issues such as data saturation or packet loss.

(2) The control of switched stochastic nonlinear pure-feedback systems proves challenging due to the non-affine linkage between inputs and states. To address this, we adopt backstepping techniques in the spirit of Ref. [23], but we incorporate dynamic surface control (DSC) to avoid repeated differentiation of virtual control signals. This approach eases the computational burden commonly associated with backstepping, enhancing design simplicity.

(3) A major element of our work is state estimation, achieved via a state observer. This differs from Ref. [24], where robust stabilization of switched systems with time-varying delays was considered under the assumption of known parameters. In our scheme, the latest available measurement is used to approximate lost data, while neural networks approximate unknown nonlinearities within the system. Both ideal and impaired measurement scenarios are examined via backstepping-based Lyapunov design, ensuring appropriate adaptive laws for different subsystems and guaranteeing stability alongside desired performance levels.

The remainder of this paper is organized as follows: In Section 2, we present the system model, including data transmission processes, average dwell time, and the radial basis function (RBF) neural network. Section 3 focuses on designing the switched estimator and backstepping control under normal and data-loss conditions. Section 4 provides the stability analysis, and Section 5 offers a simulation example. Finally, Section 6 concludes the paper.

Notations: Let $\mathbb{R}^n$ represent the n-dimensional real vector space, and I be the identity matrix of the appropriate dimension. P^T indicates the transpose of matrix or vector P. The notation $P > 0$ means P is positive definite. The Euclidean norm of a vector e is given by $\|e\|$. The largest and smallest eigenvalues of a symmetric matrix are denoted $\lambda_{\max}(\cdot)$ and $\lambda_{\min}(\cdot)$, respectively. $E[x]$ and $D[x]$ represent the expectation and variance of the random variable x. Lastly, $tr(P)$ denotes the trace of matrix P.

II. System Description and Preliminaries

We consider a class of switched stochastic nonlinear pure-feedback systems with incomplete measurements, governed by the following system dynamics:

$$\begin{aligned} &dx_i = f_{\sigma(t),i}(\bar{x}_i, x_{i+1})dt + \varphi^T_{\sigma(t),i}(x_1)dw_t, \\ &\vdots \\ &dx_n = f_{\sigma(t),n}(\bar{x}_n, u_{\sigma(t)})dt + \varphi^T_{\sigma(t),n}(x_1)dw_t, \\ &y = \rho_1 x_1 + \rho_2 \iota(x_1) + \rho_3 \varsigma(x_1), \end{aligned} \tag{1}$$

where $\bar{x}_n = [x_1, x_2, \ldots, x_n]^T \in \mathbb{R}^n$ represents the state vector of the system, and $\bar{x}_i = [x_1, x_2, \ldots, x_i]^T \in \mathbb{R}^i$ for $i = 1, 2, \ldots, n-1$, represents the vector of states from x_1 to x_i. The system output, denoted by y, is determined by the linear combination of various components. The control input for the k-th subsystem is represented as u_k. The functions $f_{k,i}(\cdot) : \mathbb{R}^{i+1} \to \mathbb{R}$ and $\varphi^T_{k,i}(\cdot) : \mathbb{R}^{i+1} \to \mathbb{R}^r$ are smooth but unknown nonlinear functions, where w_t represents an r-dimensional standard Wiener process. The switching signal $\sigma(t) : [0, \infty) \to M = \{1, 2, \ldots, m\}$ governs transitions between subsystems, with m being the total number of subsystems. The function $\iota(\cdot)$ models a saturation effect, and $\varsigma(\cdot)$ represents a data-loss function. The parameters ρ_1, ρ_2, and ρ_3 reflect different measurement scenarios, constrained by $\rho_1 + \rho_2 + \rho_3 = 1$. Specifically, $\rho_1 = 1$ corresponds to normal measurement, $\rho_2 = 1$ represents saturated measurement, and $\rho_3 = 1$ indicates lost measurement [26–28]. Note that ρ_1, ρ_2, and ρ_3 represent weighting factors for different output measurement scenarios, where only one of them is nonzero at any given time, reflecting either normal, saturated, or lost measurement.

In contrast to strict-feedback systems, the input-state relationship in pure-feedback systems is non-affine, which presents significant challenges for control law design. To address these, we apply the mean value theorem to approximate the term $f_{k,i}(\bar{x}_i, x_{i+1})$ in equation (1). This yields the following approximation:

$$f_{k,i}(\overline{x}_i, x_{i+1}) = f_{k,i}(\overline{x}_i, x^0_{i+1}) + g_{\mu i}(x_{i+1} - x^0_{i+1}), \tag{2}$$

where $g_{\mu i} = \left(\frac{\partial f_{k,i}(\overline{x}_i, x_{i+1})}{\partial x_{i+1}}\right)\Big|_{x_{i+1}=x_{\mu i}}$, and $x_{\mu i} = (1 - \mu_i)x^0_{i+1} + \mu_i x_{i+1}$, with $0 < \mu_i < 1$ for $i = 1, 2, \ldots, n$.

Additionally, we set $x_{n+1} = u$. By setting $x^0_{i+1} = 0$ and substituting equation (2) into equation (1), we obtain the following simplified system dynamics:

$$\begin{aligned} dx_i &= \left(f_{\sigma(t),i}(\bar{x}_i) + g_{\mu i} x_{i+1}\right) dt + \varphi^T_{\sigma(t),i}(x_1)dw, \\ &\vdots \\ dx_n &= \left(f_{\sigma(t),n}(\bar{x}_n) + g_{\mu n} u_{\sigma(t)}\right) dt + \varphi^T_{\sigma(t),n}(x_1)dw, \\ y &= \rho_1 x_1 + \rho_2 \iota(x_1) + \rho_3 \varsigma(x_1). \end{aligned} \tag{3}$$

In equation (3), we assume that the output measurement satisfies the condition $|x_1| \le x_{\text{max}}$, where x_{max} represents the upper bound on the state x_1.

Lemma 1: ([25]): For all $(x, y) \in \mathbb{R}^2$, the following inequality holds:

$$xy \le \frac{\varepsilon^p}{p}|x|^p + \frac{1}{q\varepsilon^q}|y|^q,$$

where $p > 1$, $q > 1$, and $(p-1)(q-1) = 1$.

To approximate the unknown nonlinear functions $f_{k,i}$ and $\varphi_{k,i}$, we employ a RBF neural network[22, 23]. The RBF network approximates these nonlinear functions by constructing a series of basis functions that are radially symmetric around a set of centroids. Specifically, the approximation takes the form:

$$f_{k,i}(\bar{x}_i) \approx \sum_{j=1}^{N} \theta_j \phi_j(\bar{x}_i), \quad \varphi_{k,i}^T(x_1) \approx \sum_{j=1}^{N} \gamma_j \phi_j(x_1), \quad (4)$$

where $\phi_j(\cdot)$ are the radial basis functions, typically chosen to be Gaussian functions, θ_j and γ_j are the corresponding network weights, and N is the number of neurons in the network. The network's structure is designed to capture the underlying nonlinearities in the system, allowing for accurate approximation of $f_{k,i}$ and $\varphi_{k,i}$, and improving the overall performance of the control system. The learning process involves updating the weights θ_j and γ_j based on the observed data and the desired system behavior, typically through a supervised learning method such as the least-squares approach.

The use of RBF networks in this context provides a flexible, data-driven approach to model the system's nonlinear dynamics, enabling the design of control laws that can handle the complexities of the switched stochastic system with incomplete measurements.

III. Main Result

The objective of this study is to develop an adaptive neural network control strategy for a switched stochastic nonlinear pure-feedback system, as described by equation (1), utilizing a state estimator based on the backstepping method. In this context, the system output is the sole available measurement, and thus, a state observer must be introduced to facilitate the design of the controller based on estimated system states. It is important to highlight that the output of system (1) is subject to disturbances arising from two primary factors: input saturation and packet loss. In the case of saturation, the system output is limited to a maximum value, denoted as $\iota(x_1)$, which corresponds to the most recent value recorded before saturation occurred. Meanwhile, when packet loss occurs, the most recent valid output is used to replace the actual output value. From an observer and controller design perspective, these two disturbance scenarios can be unified under a common framework referred to as the "data-loss scenario," in which the current observation is replaced by the last known valid output. Thus, the design of the state estimation and control strategies is examined under two distinct conditions: normal operation and data-loss events.

A. State Estimation and Backstepping Control Design Under Normal Conditions

In the normal operating mode, where the system output is available for observation, the state estimator can be constructed based on the output y. Utilizing equation (1), an observer-based controller is designed to ensure that all signals in the closed-loop system remain uniformly ultimately bounded. The state estimator for the normal case is defined as:

$$\begin{aligned}\dot{\hat{x}}_{ci} &= f_{\sigma(t),i}(\hat{x}_{ci}) + g_{\mu i}\hat{x}_{c(i+1)} \\ &\quad + l_{\sigma(t),i}(y - \hat{x}_{ci}), \quad i = 1, \ldots, n-1 \\ \dot{\hat{x}}_{cn} &= f_{\sigma(t),n}(\overline{\hat{x}}_{cn}) + g_{\mu n}u_{c,\sigma(t)} + l_{\sigma(t),n}(y - \hat{x}_{c1}), \quad (5)\end{aligned}$$

where $\overline{\hat{x}}_{ci} = [\hat{x}_{c1}, \ldots, \hat{x}_{cn}]^T \in \mathbb{R}^i$, and $\hat{x}_{ci}$ $(i = 1, 2, \ldots, n)$ represents the estimates of x_{ci} under normal conditions. The output $y = x_1$ is the observed signal of the switched system, and $u_{c,k}$ denotes the control input for the k-th subsystem under each $k \in M$. The switching signal $\sigma(t)$ is defined earlier, and $l_{k,i}, i = 1, \ldots, n, k \in M$ are the design parameters.

Let $e_c = \overline{x}_n - \overline{\hat{x}}_{cn}$ be the estimator error, where the first element is $e_{c1} = y - \hat{x}_{c1}$. By differentiating equations (1) and (2), the time derivative of the estimator error is:

$$\begin{aligned} de_c &= \dot{\overline{x}}_n - \dot{\overline{\hat{x}}}_{cn} \\ &= (A_k e_c + \Delta F_k - L_c e_{c1})dt + \varphi_k^T(x_1)dw \\ &= ((A_k - L_c C)e_c + \Delta F_k)\, dt + \varphi_k^T(x_1)dw \quad (6)\end{aligned}$$

where

$$A_k = \begin{bmatrix} 0 & g_{\mu 1} & 0 & \cdots & 0 \\ 0 & 0 & g_{\mu 2} & \cdots & 0 \\ \vdots & & & \ddots & \\ 0 & & \cdots & & g_{\mu(n-1)} \\ 0 & & \cdots & & 0 \end{bmatrix}$$

Here, $L_c = [l_{k,1}, \ldots, l_{k,n}]^T$, $C = [1, 0, \ldots, 0]$, and $\Delta F_k = [\Delta F_{k,1}, \ldots, \Delta F_{k,n}]^T$, where $\Delta F_{k,i} = f_{k,i}(\overline{x}_i) - f_{k,i}(\overline{\hat{x}}_{ci})$. The term $\varphi_k(x_1)$ is defined as $\varphi_k(x_1) = [\varphi_{k,1}(x_1), \ldots, \varphi_{k,n}(x_1)]$.

To evaluate the stability of the estimation error $e_c = \overline{x}_n - \overline{\hat{x}}_{cn}$, we define the candidate Lyapunov function as $V_{c0} = \frac{1}{2}(e_c^T P e_c)^2$, where P is a positive definite matrix to be determined. The time derivative of V_{c0} along the trajectory of equation (5) is:

$$\begin{aligned}\dot{V}_{c0} &= e_c^T P e_c \left(2e_c^T P \left((A_k - L_c C)e_c + \Delta F_{\sigma(t)}\right)\right) \\ &\quad + \frac{1}{2}\mathrm{tr}\left(\varphi_k^T \left(4Pe_c e_c^T P + 2e_c^T P e_c P\right)\varphi_k\right)\end{aligned} \quad (7)$$

B. Parameter Selection and Stability Analysis

In order to ensure the stability of the system, it is necessary to select the parameter vector L such that $(A_k - L_c C)$ is a strictly Hurwitz matrix. Assuming the existence of a positive definite symmetric matrix $Q > 0$, there is a corresponding positive definite symmetric matrix $P > 0$ such that Q can be expressed as $Q = -(P(A_k - L_c C) + (A_k - L_c C)^T P)$. Let $\lambda = \lambda_{\min}(P)\lambda_{\min}(Q)$, then the following inequality is satisfied:

$$e_c^T P e_c \left(e_c^T \left(P(A_k - L_c C) + (A_k - L_c C)^T P\right) e_c\right) \leq -\lambda_c \|e_c\|^4 \quad (8)$$

Using Assumption 2 and Lemma 1, we obtain $\|f_{\sigma(t),i}(\bar{x}_i) - f_{\sigma(t),i}(\bar{\hat{x}}_{ci})\| \leq m_i \|e_c\|$, resulting in

$$\begin{aligned} & 2e_c^T P e_c e_c^T P \Delta F_k \leq 2\|e_c\|\|P\|\|e_c\|\|e_c\|\|P\|\|\Delta F_k\| \\ = \ & 2\|e_c\|^3 \|P\|^2 \|\Delta F_k\| \\ \leq \ & 2\sqrt{\sum_{i=1}^{n} m_i^2 \|P\|^2 \|e_c\|^4} \quad (9)\end{aligned}$$

For the trace term, we have

$$\begin{aligned}
& \operatorname{tr}(\varphi_k^T(x_1)(2Pe_ce_c^TP + e_c^TPe_cP)\varphi_k(x_1)) \\
\leq\ & n\|\varphi_k^T(x_1)(2Pe_ce_c^TP + e_c^TPe_cP)\varphi_k(x_1)\|_F \\
\leq\ & n\sqrt{n}\|\varphi_k^T(x_1)(2Pe_ce_c^TP + e_c^TPe_cP)\varphi_k(x_1)\| \\
\leq\ & 3n\sqrt{n}\|\varphi_k(x_1)\|^2\|P\|^2\|e_c\|^2 \\
\leq\ & \frac{3n\sqrt{n}}{2\eta_{c0}^2}\|P\|^4\|e_c\|^4 + \frac{3n\sqrt{n}\eta_{c0}^2}{2}\|\varphi_k(x_1)\|^4 \quad (10)
\end{aligned}$$

where η_{c0} is a positive design parameter.

Substituting (12)-(14) into (7) yields

$$LV_{c0} \leq -p_{c0}\|e_c\|^4 + \frac{3n\sqrt{n}\eta_{c0}^2}{2}x_1^4\|\psi_k(x_1)\|^4 \quad (11)$$

where $p_{c0} = \lambda_c - 2\sqrt{\sum_{i=1}^n m_i^2}\|P\|^2 - \frac{3n\sqrt{n}}{2\eta_{c0}^2}\|P\|^4$.

C. Control Signal Construction

For each $i = 1, 2, \ldots, n$, the RBF neural network $W_{cki}^T S_{ci}(Z_{ci})$ is utilized to approximate the unknown nonlinear function $\bar{f}_{ci}(Z_{ci})$ at each step. The virtual control signal and actual control input are formulated as follows:

$$\alpha_{cki}(Z_{ci}) = -l_i^c Z_{ci} - \frac{1}{2a_{ci}^2}Z_{ci}^3\hat{\theta}_c S_{ci}^T(Z_{ci})S_{ci}(Z_{ci}), \quad (12)$$

$$u_{c,k}(Z_n) = -l_n^c Z_{cn} - \frac{1}{2a_{cn}^2}Z_{cn}^3\hat{\theta}_{cn} S_{cn}^T(Z_{cn})S_{cn}(Z_{cn}) \quad (13)$$

where l_i^c and $a_{ci}\,(i = 1, 2, \ldots, n)$ are positive design constants, and $S_{ci}(Z_{ci})$ is the basis function vector with $Z_{ci} = [\bar{x}_{ci}^T, \hat{\theta}_c]^T \in \Omega_{Z_{ci}} \subset \mathbb{R}^{i+1}$ for $i = 1, \ldots, n$.

Define the constant θ_c as:

$$\theta_c = \max\left\{\frac{1}{d_m}\|W_{cki}\|^2 : k \in M\right\}, \quad (14)$$

where d_m is given in Assumption 1. Since the constant $\|W_{cki}\|$ is not known, θ_c remains unknown as well. The parameter error is denoted as $\widetilde{\theta}_c = \theta_c - \hat{\theta}_c$, representing the estimate error of θ_c.

The adaptive law is given by:

$$\dot{\hat{\theta}}_c = \sum_{i=1}^n \frac{r}{2a_{ci}^2}Z_{ci}^6 S_{ci}^T(Z_{ci})S_{ci}(Z_{ci}) - \bar{l}_0^c\hat{\theta}_c, \quad 1 \leq i \leq n, \quad (15)$$

where $a_{ci}\,(i = 1, \ldots, n)$ and $\bar{l}_0^c$ are positive design parameters.

Using this adaptive law, the backstepping method is applied to derive the actual control law. This process consists of n steps: from the first step to the $(n-1)$th step, the virtual control α_{ci} is designed, and in the nth step, the actual control input u is obtained. To simplify the following derivations, the time variable t is omitted, and for convenience, we set $S_{ci}(Z_{ci}) = S_{ci}$.

To mitigate the complexity explosion, the dynamic surface control (DSC) method is introduced, which incorporates a coordinate transformation in the backstepping design. The transformation is as follows:

$$\begin{aligned}
Z_{c1} &= x_1, \\
Z_{ci} &= \hat{x}_{ci} - \alpha_{cif}, \\
\chi_{ci} &= \alpha_{cif} - \alpha_{c(i-1)}, \quad i = 2, 3, \ldots, n, \quad (16)
\end{aligned}$$

where Z_{c1} represents the error surface, χ_{ci} is the output error of the first-order filter, and α_{cif} is the output of the first-order filter with $\alpha_{c(i-1)}$ as the input.

To avoid repetitive differentiation of $\alpha_{ck(i-1)}$ for $i = 2, \ldots, n$, we introduce a new state variable α_{cif}. The variable $\alpha_{ck(i-1)}$ is passed through a first-order filter with time constant κ_{ci} to obtain α_{cif}, as follows:

$$\begin{aligned}
&\kappa_{ci}\dot{\alpha}_{cif} + \alpha_{cif} = \alpha_{ck(i-1)}, \\
&\qquad \alpha_{cif}(0) = \alpha_{ck(i-1)}(0), \quad i = 2, \ldots, n.
\end{aligned} \quad (17)$$

Let $\chi_{ci} = \alpha_{cif} - \alpha_{ck(i-1)}$ denote the output error of the filter. Thus, we have $\dot{\alpha}_{cif} = -\chi_{ci}/\kappa_{ci}$, and the dynamics for χ_{ci} are given by:

$$\dot{\chi}_{ci} = \dot{\alpha}_{cif} - \dot{\alpha}_{ck(i-1)} = -\frac{\chi_{ci}}{\kappa_{ci}} + B_{ci}(X_{i-1}), \quad (18)$$

where:

$$B_{ci}(X_{i-1}) = l_i^c\dot{Z}_{ci} + \frac{3}{2a_{ci}^2}Z_{ci}^2\dot{Z}_{ci}\hat{\theta}_c S_{ci}^T(Z_{ci})S_{ci}(Z_{ci}), \quad (19)$$

Using Ito's differentiation rule, we have:

$$\begin{aligned}
dZ_{c1} &= (f_{k,1}(x_1) + g_{\mu 1}x_2)dt + \varphi_{k,1}^T(x_1)dw, \\
dZ_{ci} &= (f_{k,i}(\bar{\hat{x}}_{ci}) + g_{\mu i}\hat{x}_{c(i+1)} + l_{k,1}(y - \hat{x}_{c1}) \\
&\quad - \dot{\alpha}_{cif})dt, \quad i = 2, 3, \ldots, n. \quad (20)
\end{aligned}$$

Step 1: Consider the Lyapunov function:

$$V_{c1} = V_{c0} + \frac{1}{4}Z_{c1}^4 + \frac{d_m}{2r}\widetilde{\theta}_c^2. \quad (21)$$

Differentiating V_{c1} yields:

$$\begin{aligned}
LV_{c1} &= LV_{c0} + Z_{c1}^3\left(f_{k,1}(x_1) + g_{\mu 1}x_2\right) \\
&\quad + \frac{1}{2}\operatorname{tr}\left(\varphi_{k,1}^T(x_1)3Z_{c1}^2\varphi_{k,1}(x_1)\right) \\
&\quad - \frac{d_m}{r}\widetilde{\theta}_c\dot{\hat{\theta}}_c, \\
&= LV_{c0} + Z_{c1}^3\left(f_{k,1}(x_1) + g_{\mu 1}\hat{x}_{c2} + g_{\mu 1}e_{c2}\right) \\
&\quad + \frac{3}{2}\operatorname{tr}\left(\varphi_{k,1}^T(x_1)Z_{c1}^2\varphi_{k,1}(x_1)\right) \\
&\quad - \frac{d_m}{r}\widetilde{\theta}_c\dot{\hat{\theta}}_c. \quad (22)
\end{aligned}$$

Using Young's inequality, the following holds:

$$\begin{aligned}
g_{\mu 1}Z_{c1}^3 e_{c2} &\leq \frac{3}{4}d_M\eta_{c1}^{\frac{4}{3}}Z_{c1}^4 + \frac{1}{4\eta_{c1}^4}d_M e_{c2}^4 \\
&\leq \frac{3}{4}d_M\eta_{c1}^{\frac{4}{3}}Z_{c1}^4 + \frac{1}{4\eta_{c1}^4}d_M\|e_c\|^4, \\
\frac{1}{2}&\operatorname{tr}\left(\varphi_{k,1}^T(x_1)3Z_{c1}^2\varphi_{k,1}(x_1)\right) \\
&\leq \frac{3}{4}\eta_{c2}^2 Z_{c1}^4\|\psi_{k,1}(x_1)\|^4 + \frac{3}{4\eta_{c2}^2}, \quad (23)
\end{aligned}$$

where η_{c1} and η_{c2} are positive constants to be designed. By substituting these results into Eq. (22), we have:

$$\begin{aligned}
LV_{c1} &\leq -p_{c1}\|e_c\|^4 + Z_{c1}^3(g_{\mu 1}\hat{x}_{c2} + \overline{f}_{c1}(Z_{c1})) \\
&\quad - \frac{3}{4}Z_{c1}^4 - \frac{d_m}{r}\widetilde{\theta}_c\dot{\hat{\theta}}_c + \frac{3}{4\eta_{c2}^2}, \quad (24)
\end{aligned}$$

where

$$p_{c1} = p_{c0} - \frac{1}{4\eta_{c1}^4} d_M,$$
$$\overline{f}_{c1}(Z_{c1}) = f_{k,1} + \left(\frac{3n\sqrt{n}\eta_{c0}^2}{2} \|\psi_{k,1}(x_1)\|^4 + \frac{3}{4} d_M \eta_{c1}^{4/3} + \frac{3}{4}\eta_{c2}^2 \|\psi_{k,1}(x_1)\|^4 + \frac{3}{4} \right) Z_{c1}.$$

Since $\overline{f}_{c1}$ contains unknown functions $f_{k,1}$ and $\|\psi_{k,1}(x_1)\|$, the RBF neural network $W_{ck1}^T S_{c1}(Z_{c1})$ can be used to approximate $\overline{f}_{c1}$ with an approximation error $\delta_{ck1}(Z_{c1})$ such that:

$$\overline{f}_{c1} = W_{ck1}^T S_{c1}(Z_{c1}) + \delta_{ck1}(Z_{c1}), \quad |\delta_{ck1}(Z_{c1})| \le \varepsilon_{c1},$$

where $\varepsilon_{c1} > 0$ is a given constant. Using Young's inequality, we have:

$$\begin{aligned} Z_{c1}^3 \overline{f}_{c1} &= Z_{c1}^3 \frac{W_{ck1}^T}{\|W_{ck1}\|} \|W_{ck1}\| S_{c1} + Z_{c1}^3 \delta_{ck1}(Z_{c1}) \\ &\le \frac{1}{2a_{c1}^2} Z_{c1}^6 \|W_{ck1}\|^2 S_{c1}^T S_{c1} + \frac{1}{2}a_{c1}^2 + \frac{3}{4}Z_{c1}^4 + \frac{1}{4}\varepsilon_{c1}^4 \\ &\le \frac{d_m}{2a_{c1}^2} Z_{c1}^6 \theta_c S_{c1}^T S_{c1} + \frac{1}{2}a_{c1}^2 + \frac{3}{4}Z_{c1}^4 + \frac{1}{4}\varepsilon_{c1}^4, \quad (25) \end{aligned}$$

where a_{c1} is a positive design parameter and θ_c is defined in Eq. (14). Substituting Eq. (25) into Eq. (22) yields:

$$\begin{aligned} LV_{c1} \le& -p_{c1}\|e_c\|^4 + g_{\mu 1} Z_{c1}^3 \hat{x}_{c2} + \frac{d_m}{2a_{c1}^2} Z_{c1}^6 \theta_c S_{c1}^T S_{c1} \\ &+ \frac{1}{2}a_{c1}^2 + \frac{1}{4}\varepsilon_{c1}^4 - \frac{d_m}{r}\widetilde{\theta}_c \dot{\hat{\theta}}_c + \frac{3}{4\eta_{c2}^2}. \end{aligned} \quad (26)$$

Adding and subtracting α_{c1} and using the coordinate transformation in Eq. (16) with $i = 2$, we have:

$$\begin{aligned} LV_{c1} \le& -p_{c1}\|e_c\|^4 + g_{\mu 1} Z_{c1}^3 (Z_{c2} + \alpha_{c2f} - \alpha_{c1}) \\ &+ g_{\mu 1} Z_{c1}^3 \alpha_{c1} + g_{\mu 1} Z_{c1}^3 \alpha_{ck1} \\ &+ \frac{d_m}{2a_{c1}^2} Z_{c1}^6 \theta_c S_{c1}^T S_{c1} - \frac{d_m}{r}\widetilde{\theta}_c \dot{\hat{\theta}}_c \\ &+ \frac{3}{4\eta_{c2}^2}. \end{aligned} \quad (27)$$

By constructing the virtual control signal α_{ck1} in Eq. (31) for $i = 1$ and applying Assumption 1[16], we have:

$$g_{\mu 1} Z_{c1}^3 \alpha_{ck1} \le -l_1^c g_{\mu 1} Z_{c1}^4 - \frac{d_m}{2a_{c1}^2} Z_{c1}^6 \hat{\theta}_c S_{c1}^T S_{c1}. \quad (28)$$

Combining the previous results, we obtain:

$$\begin{aligned} LV_{c1} \le& -p_{c1}\|e_c\|^4 - C_{c1} Z_{c1}^4 + g_{\mu 1} Z_{c1}^3 (Z_{c2} + \chi_{c1}) \\ &- \frac{d_m}{r}\widetilde{\theta}_c \left(\frac{r}{2a_{c1}^2} Z_{c1}^6 \hat{\theta}_c S_{c1}^T S_{c1} - \dot{\hat{\theta}}_c \right) + \Delta_{c1}, \end{aligned} \quad (29)$$

where $C_{c1} = l_1^c g_{\mu 1} > 0$ and $\Delta_{c1} = \frac{3}{4\eta_{c2}^2} + \frac{1}{2}a_{c1}^2 + \frac{1}{4}\varepsilon_{c1}^4$.

Step m ($2 \le i \le n-1$): Consider the Lyapunov function candidate:

$$V_{ckm} = V_{ck(m-1)} + \frac{1}{4}Z_{cm}^4 + \frac{1}{4}\chi_{cm}^4. \quad (30)$$

Similarly, we have:

$$\begin{aligned} LV_{cm} \le& -p_{c1}\|e_c\|^4 - \sum_{i=1}^{m-1} C_{ci} Z_{ci}^4 + Z_{cm}^3 (g_{\mu m}\hat{x}_{c(m+1)} + \overline{f}_{cm}) \\ &+ \sum_{i=1}^{m-1} g_{\mu i} Z_{ci}^3 (Z_{c(i+1)} + \chi_{c(i+1)}) \\ &+ \sum_{i=1}^{m-1} \left(\frac{\chi_{c(i+1)}^4}{\kappa_{c(i+1)}} - \chi_{c(i+1)}^3 B_{c(i+1)}(X_i) \right) \\ &- \frac{d_m}{r}\widetilde{\theta}_c \left(\sum_{i=1}^{m-1} \frac{r}{2a_{ci}^2} Z_{ci}^6 \hat{\theta}_c S_{ci}^T S_{ci} - \dot{\hat{\theta}}_c \right) \\ &- \frac{3}{4}Z_{cm}^4 + \Delta_{c(m-1)}, \end{aligned} \quad (31)$$

where $\overline{f}_{cm} = (f_{k,m} + l_{k,m} e_{c1} - \dot{\alpha}_{cmf}) + \frac{3}{4}Z_{cm}$.

Similar to Step 1, $\overline{f}_{cm}$ contains an unknown function. Given any constant $\varepsilon_{cm} > 0$, the RBF neural network $W_{ckm}^T S_{cm}(Z_{cm})$ is used to approximate $\overline{f}_{cm}$,

$$\overline{f}_{cm} = W_{ckm}^T S_{cm}(Z_{cm}) + \delta_{ckm}(Z_{cm}), \quad |\delta_{ckm}(Z_{cm})| \le \varepsilon_{cm},$$

where $\delta_{ckm}(Z_{cm})$ represents the approximation error, and $Z_i = [\bar{x}_i^T, \widetilde{\theta}_c]^T$. Applying Young's inequality, we have

$$Z_{cm}^3 \overline{f}_{cm} \le \frac{d_m}{2a_{cm}^2} Z_{cm}^6 \theta_c S_{cm}^T S_{cm} + \frac{1}{2}a_{cm}^2 + \frac{3}{4}Z_{cm}^4 + \frac{1}{4}\varepsilon_{cm}^4. \quad (32)$$

Combining this result with Eq. (33) gives

$$\begin{aligned} LV_{cm} \le& -p_{c1}\|e_c\|^4 - \sum_{i=1}^{m-1} C_{ci} Z_{ci}^4 + g_{\mu m} Z_{cm}^3 \hat{x}_{c(m+1)} \\ &+ \sum_{i=1}^{m-1} g_{\mu i} Z_{ci}^3 (Z_{c(i+1)} + \chi_{c(i+1)}) \\ &+ \sum_{i=1}^{m-1} \left(\frac{\chi_{c(i+1)}^4}{\kappa_{c(i+1)}} - \chi_{c(i+1)}^3 B_{c(i+1)}(X_i) \right) \\ &+ \Delta_{c(m-1)} + \frac{d_m}{2a_{cm}^2} Z_{cm}^6 \theta_c S_{cm}^T S_{cm} \\ &- \frac{d_m}{r}\widetilde{\theta}_c \left(\sum_{i=1}^{m-1} \frac{r}{2a_{ci}^2} Z_{ci}^6 \hat{\theta}_c S_{ci}^T S_{ci} - \dot{\hat{\theta}}_c \right) \\ &+ \frac{1}{2}a_{cm}^2 + \frac{1}{4}\varepsilon_{cm}^4. \end{aligned} \quad (33)$$

Next, by constructing the virtual control signal α_{cm} in Eq. (35) and following a similar procedure using the coordinate transformation in Eq. (20) with $i = m+1$, we obtain:

$$\begin{aligned} LV_{cm} \le & -p_{c1}\|e_c\|^4 \\ & - \sum_{i=1}^{m-1} C_{ci} Z_{ci}^4 + g_{\mu m} Z_{cm}^3 (Z_{c(m+1)} \\ & + \alpha_{c(m+1)f} - \alpha_{ckm}) \\ & + g_{\mu m} Z_{cm}^3 \alpha_{ckm} + \sum_{i=1}^{m-1} g_{\mu i} Z_{ci}^3 (Z_{c(i+1)} + \chi_{c(i+1)}) \\ & + \sum_{i=1}^{m-1} \left(\frac{\chi_{c(i+1)}^4}{\kappa_{c(i+1)}} - \chi_{c(i+1)}^3 B_{c(i+1)}(X_i) \right) \\ & + \Delta_{c(m-1)} + \frac{d_m}{2a_{cm}^2} Z_{cm}^6 \theta_c S_{cm}^T S_{cm} \\ & - \frac{d_m}{r} \widetilde{\theta}_c \left(\sum_{i=1}^{m-1} \frac{r}{2a_{ci}^2} Z_{ci}^6 \hat{\theta}_c S_{ci}^T S_{ci} \right) \\ & + \frac{d_m}{r} \widetilde{\theta}_c \dot{\hat{\theta}}_c + \frac{1}{2} a_{cm}^2 + \frac{1}{4} \varepsilon_{cm}^4. \end{aligned} \tag{38}$$

Using Assumption 1[16] and constructing the virtual control signal α_{ckm} in Eq. (31) for $i = m$, we have:

$$g_{\mu m} Z_{cm}^3 \alpha_{ckm} \le -l_m^c g_{\mu m} Z_{cm}^4 - \frac{d_m}{2a_{cm}^2} Z_{cm}^6 \hat{\theta}_c S_{cm}^T S_{cm}. \tag{34}$$

Combining these results, we get:

$$\begin{aligned} LV_{cm} \le & -p_{c1}\|e_c\|^4 - \sum_{i=1}^{m} C_{ci} Z_{ci}^4 \\ & + \sum_{i=1}^{m} g_{\mu i} Z_{ci}^3 (Z_{c(i+1)} + \chi_{c(i+1)}) \\ & + \sum_{i=1}^{m-1} \left(\frac{\chi_{c(i+1)}^4}{\kappa_{c(i+1)}} - \chi_{c(i+1)}^3 B_{c(i+1)}(X_i) \right) \\ & - \frac{d_m}{r} \widetilde{\theta}_c \left(\sum_{i=1}^{m} \frac{r}{2a_{ci}^2} Z_{ci}^6 \hat{\theta}_c S_{ci}^T S_{ci} - \dot{\hat{\theta}}_c \right) + \Delta_{cm}, \end{aligned} \tag{35}$$

where $C_{ci} = l_i^c g_{\mu i} > 0$, and

$$\Delta_{cm} = \frac{3}{4\eta_{c2}^2} + \frac{1}{2} \sum_{i=1}^{m} \left(a_{ci}^2 + \frac{1}{2} \varepsilon_{ci}^4 \right). \tag{36}$$

Step n: Consider the following Lyapunov function:

$$V_{ckn} = V_{ck(n-1)} + \frac{1}{4} Z_{cn}^4 + \frac{1}{4} \chi_{cn}^4 + \frac{d_m}{2r} \widetilde{\theta}_{cn}^2. \tag{37}$$

Similarly, we obtain:

$$\begin{aligned} LV_{cn} \le & -p_{c1}\|e_c\|^4 - \sum_{i=1}^{n-1} C_{ci} Z_{ci}^4 + Z_{cn}^3 (g_{\mu n} u_{c,k} + \overline{f}_{cn}) \\ & + \sum_{i=1}^{n-1} g_{\mu i} Z_{ci}^3 (Z_{c(i+1)} + \chi_{c(i+1)}) \\ & + \sum_{i=1}^{n-1} \left(\frac{\chi_{c(i+1)}^4}{\kappa_{c(i+1)}} - \chi_{c(i+1)}^3 B_{c(i+1)}(X_i) \right) \\ & - \frac{d_m}{r} \widetilde{\theta}_c \left(\sum_{i=1}^{n-1} \frac{r}{2a_{ci}^2} Z_{ci}^6 \hat{\theta}_c S_{ci}^T S_{ci} - \dot{\hat{\theta}}_c \right) \\ & - \frac{3}{4} Z_{cn}^4 + \Delta_{c(n-1)}, \end{aligned} \tag{38}$$

where

$$\overline{f}_{cn} = f_{k,n} + l_{k,n} e_{c1} - \dot{\alpha}_{cnf} + \frac{3}{4} Z_{cn}. \tag{39}$$

Similar to the above steps, the RBF neural network $W_{ckn}^T S_{cn}(Z_{cn})$ is used to approximate the unknown nonlinear function $\overline{f}_{cn}$:

$$\overline{f}_{cn}(Z_{cn}) = W_{ckn}^T S_{cn}(Z_{cn}) + \delta_{ckn}(Z_{cn}), \quad |\delta_{ckn}(Z_{cn})| \le \varepsilon_{cn},$$

where $\delta_{ckn}(Z_{cn})$ is the approximation error, and $\varepsilon_{cn} > 0$ is an arbitrary constant. Thus, we have

$$Z_{cn} \overline{f}_{cn} \le \frac{d_m}{2a_{cn}^2} Z_{cn}^6 \theta_{cn} S_{cn}^T S_{cn} + \frac{1}{2} a_{cn}^2 + \frac{3}{4} Z_{cn}^4 + \frac{1}{4} \varepsilon_{cn}^2, \tag{40}$$

where $a_{cn} > 0$ is a design parameter. Substituting (41) into (40), we get

$$\begin{aligned} LV_{cn} \le & -p_{c1}\|e_c\|^4 - \sum_{i=1}^{n-1} C_{ci} Z_{ci}^4 + Z_{cn}^3 g_{\mu n} u_{c,k} \\ & + \frac{d_m}{2a_{cn}^2} Z_{cn}^6 \theta_{cn} S_{cn}^T S_{cn} \\ & + \sum_{i=1}^{n-1} g_{\mu i} Z_{ci}^3 (Z_{c(i+1)} + \chi_{c(i+1)}) \\ & + \sum_{i=1}^{n-1} \left(\frac{\chi_{c(i+1)}^4}{\kappa_{c(i+1)}} - \chi_{c(i+1)}^3 B_{c(i+1)}(X_i) \right) \\ & - \frac{d_m}{r} \widetilde{\theta}_c \left(\sum_{i=1}^{n-1} \frac{r}{2a_{ci}^2} Z_{ci}^6 \hat{\theta}_c S_{ci}^T S_{ci} - \dot{\hat{\theta}}_c \right) \\ & + \frac{1}{2} a_{cn}^2 + \frac{1}{4} \varepsilon_{cn}^2 + \Delta_{c(n-1)} \end{aligned} \tag{41}$$

Following a similar procedure, by using the definition of $u_{c,k}$ in (17) and applying Lemma 1, we obtain

$$g_{\mu n} Z_{cn}^3 u_{c,k} \le -l_n^c g_{\mu n} Z_{cn}^4 - \frac{d_m}{2a_{cn}^2} Z_{cn}^6 \hat{\theta}_c S_{cn}^T S_{cn} \tag{42}$$

Substituting (43) into (42), we get

$$\begin{aligned} LV_{cn} \le & -p_{c1}\|e_c\|^4 - \sum_{i=1}^{n} C_{ci} Z_{ci}^4 \\ & + \sum_{i=1}^{n-1} g_{\mu i} Z_{ci}^3 (Z_{c(i+1)} + \chi_{c(i+1)}) \\ & + \sum_{i=1}^{n-1} \left(\frac{\chi_{c(i+1)}^4}{\kappa_{c(i+1)}} - \chi_{c(i+1)}^3 B_{c(i+1)}(X_i) \right) \\ & - \frac{d_m}{r} \widetilde{\theta}_c \left(\sum_{i=1}^{n} \frac{r}{2a_{ci}^2} Z_{ci}^6 \hat{\theta}_c S_{ci}^T S_{ci} - \dot{\hat{\theta}}_c \right) + \Delta_{cn} \end{aligned} \tag{43}$$

where

$$\Delta_{cn} = \frac{3}{4\eta_{c2}^2} + \frac{d_m}{2} \sum_{i=1}^{n} \left(a_{ci}^2 + \frac{1}{2} \varepsilon_{ci}^4 \right). \tag{44}$$

Now, considering the adaptive law $\dot{\hat{\theta}}_c$ in (19), the resulting equation becomes

$$\begin{aligned}LV_{cn} \leq& -p_{c1}\|e_c\|^4 - \sum_{i=1}^{n} C_{ci} Z_{ci}^4 \\ &+ \sum_{i=1}^{n-1} g_{\mu i} Z_{ci}^3 (Z_{c(i+1)} + \chi_{c(i+1)}) \\ &+ \sum_{i=1}^{n-1} \left(\frac{\chi_{c(i+1)}^4}{\kappa_{c(i+1)}} - \chi_{c(i+1)}^3 B_{c(i+1)}(X_i) \right) \\ &- \frac{d_m \bar{l}_0^c}{r} \widetilde{\theta}_c \hat{\theta}_c + \Delta_{cn} \end{aligned} \tag{45}$$

Applying Young's inequality, we have

$$\begin{aligned} g_{\mu i} Z_{ci}^3 Z_{c(i+1)} &\leq \frac{3}{4} d_M Z_{ci}^4 + \frac{1}{4} d_M Z_{c(i+1)}^4 \\ Z_{ci}^3 \chi_{c(i+1)} &\leq \frac{1}{4} d_M Z_{ci}^4 + \frac{1}{4} d_M \chi_{c(i+1)}^4 \\ |\chi_{c(i+1)}^3 B_{c(i+1)}| &\leq \frac{3}{4} \pi_c^{\frac{4}{3}} B_{c(i+1)}^{\frac{4}{3}} \chi_{c(i+1)}^4 + \frac{1}{4\pi_c^4} \\ \widetilde{\theta}_c \hat{\theta}_c = \widetilde{\theta}_c (\theta_c - \widetilde{\theta}_c) &\leq -\frac{1}{2} \widetilde{\theta}_c^2 + \frac{1}{2} \theta_c^2 \end{aligned} \tag{46}$$

where $\pi_c > 0$ is a design constant and $B_{c(i+1)}$ is a continuous function. Thus, there exists a positive constant d_{m+1} such that $|B_{c(i+1)}| \leq d_{m+1}$. Substituting (46) into (45), we get

$$\begin{aligned} LV_{cn} \leq& -p_{c1}\|e_c\|^4 \\ &- \sum_{i=1}^{n} \left(C_{ci} - \frac{7}{4} d_M \right) Z_{ci}^4 \\ &+ \sum_{i=1}^{n-1} \left(\frac{1}{\kappa_{c(i+1)}} - \frac{1}{4} d_M \right. \\ &\left. - \frac{3}{4} \pi_c^{\frac{4}{3}} B_{c(i+1)}(X_i) \right) \chi_{c(i+1)}^4 \\ &- \frac{d_m \bar{l}_0^c}{2r} \widetilde{\theta}_c^2 + \overline{\Delta}_{cn} \end{aligned} \tag{47}$$

where $C_{ci} - \frac{7}{4} d_M > 0$, and

$$\overline{\Delta}_{cn} = \Delta_{cn} + \frac{d_m \bar{l}_0^c}{2r} \theta_c^2. \tag{48}$$

D. State Estimator and Backstepping Control Design in the Presence of Data Loss

In scenarios where data loss occurs due to transmission disruptions, the available data may no longer be deemed reliable for use. Rather than discarding this corrupted data entirely, a more effective approach is to replace the missing data with prior observations from the system's routine operations. In such cases, the output x_1 may differ from the system output y. To quantify this discrepancy, we define the estimation errors as $e_{si} = x_i - \hat{x}_{si}, \quad i = 1, 2, \ldots, n$, and $e'_{s1} = x'_1 - \hat{x}_{s1}$, where $\Delta e_{s1} = e_{s1} - e'_{s1} = x_1 - x'_1$ represents the deviation between the current and the previous observations. Here, $\hat{x}_{si}$ $(i = 1, 2, \ldots, n)$ denotes the estimates of the state variables in the presence of data loss, while x'_1 is the previously observed normal output.

To address the issue of data loss, a switched estimator approach can be employed, as described by the following equations:

$$\begin{aligned} \dot{\hat{x}}_{si} &= f_{k,i}(\hat{x}_{si}) + g_{\mu i} \hat{x}_{s(i+1)} + d_m l_{\sigma(t),i}(x'_1 - \hat{x}_{s1}), \\ &\qquad i = 1, 2, \ldots, n-1, \\ \dot{\hat{x}}_{sn} &= f_{k,n}(\hat{\bar{x}}_{sn}) + g_{\mu n} u_{s,\sigma(t)} + d_m l_{\sigma(t),n}(x'_1 - \hat{x}_{s1}), \end{aligned} \tag{49}$$

In these expressions, $\hat{\bar{x}}_{si} = [\hat{x}_{s1}, \ldots, \hat{x}_{sn}]^T \in \mathbb{R}^i$ represents the vector of estimated states for each i. The system output is given by $y = x_1$, and $u_{s,k}$ is the control input for the k-th subsystem in normal operating conditions. The switching signal $\sigma(t)$ is as defined previously, and $l_{k,i}$ for $i = 1, \ldots, n$ and $k \in M$ are the controller design parameters.

To quantify the estimation error in the context of data loss, we define the error as $e_s = \bar{x}_n - \hat{\bar{x}}_{sn}$, where $\bar{x}_n$ is the true state vector, and $\hat{\bar{x}}_{sn}$ is the state estimate. From the earlier system dynamics (equations (3) and (48)), the time derivative of the estimation error can be written as:

$$\begin{aligned} de_s &= (A_k e_s + \Delta F_k - L_s e'_{s1}) dt + \varphi_k^T(x_1) dw \\ &= (A_k e_s + \Delta F_k - L_s e_{s1} + L_s \Delta e_{s1}) dt + \varphi_k^T(x_1) dw \\ &= ((A_k - L_s C) e_s + L_s \Delta e_{s1} + \Delta F_k) dt + \varphi_k^T(x_1) dw, \end{aligned} \tag{50}$$

where the matrices involved are defined as follows:

$$A_k = \begin{bmatrix} 0 & g_{\mu 1} & 0 & \ldots & 0 \\ 0 & 0 & g_{\mu 2} & \cdots & 0 \\ \vdots & & & \ddots & \\ 0 & & \ldots & & g_{\mu, n-1} \\ 0 & & \ldots & & 0 \end{bmatrix}, \tag{51}$$

$$\begin{aligned} L_s &= [d_m l_{k,1}, \ldots, d_m l_{k,n}]^T, \\ C &= [1, 0, \ldots, 0], \\ \Delta F_k &= [\Delta F_{k,1}, \ldots, \Delta F_{k,n}]^T, \quad \Delta F_{k,i} = f_{k,i}(\bar{x}_i) - f_{k,i}(\hat{\bar{x}}_{si}), \\ \varphi_k &= [\varphi_{k,1}, \ldots, \varphi_{k,n}]. \end{aligned} \tag{52}$$

Assume that h is a constant for which the following condition holds[16]:

$$\|L_s \Delta e_{s1}\| \leq h, \quad h > 0,$$

holds true.

In order to analyze the stability of the estimation error $e_s = \bar{x}_n - \hat{\bar{x}}_{sn}$, we define a candidate Lyapunov function as $V_{s0} = \frac{1}{2}(e_s^T P e_s)^2$, where P is a positive definite matrix to be determined. The time derivative of this function is computed as:

$$\begin{aligned} \dot{V}_{s0} =& e_s^T P e_s \Big(e_s^T \big(P(A_k - L_s C) + (A_k - L_s C)^T P \big) e_s \\ &+ 2 e_s^T P L_s \Delta e_{s1} + 2 e_s^T P \Delta F_k \Big) \\ &+ \frac{1}{2} \mathrm{tr} \left(\varphi_k^T(x_1) \left(4 P e_s e_s^T P + 2 e_s^T P e_s P \right) \varphi_k(x_1) \right). \end{aligned} \tag{53}$$

Using Assumptions 2 and 3[16], we deduce that the following relationship holds:

$$\|f_{\sigma(t),i}(\bar{x}_i) - f_{\sigma(t),i}(\hat{\bar{x}}_{si})\| \leq m_i \|e_s\|,$$

where the error term e_s is defined as $e_s = \overline{x}_n - \overline{\hat{x}}_{sn}$. By applying Young's inequality, we derive the following expressions:

$$2e_s^T P e_s e_s^T P \Delta F_k \leq 2\sqrt{\sum_{i=1}^{n} m_i^2 \|P\|^2} \|e_s\|^4, \tag{54}$$

$$2e_s^T P e_s e_s^T P L_s \Delta e_{s1} \leq \frac{3}{2}\eta_{s0}^{\frac{4}{3}} \|P\|^{\frac{8}{3}} \|e_s\|^4 + \frac{1}{2\eta_{s0}^4} h^4, \tag{55}$$

where η_{s0} is a positive design parameter. Additionally, by utilizing the properties of trace and norm functions, we obtain the following result:

$$\begin{aligned}
&\operatorname{tr}\left(\varphi_k^T(x_1)\left(2Pe_s e_s^T P + e_s^T P e_s P\right)\varphi_k(x_1)\right) \\
&\leq n\|\varphi_k^T(x_1)\left(2Pe_s e_s^T P + e_s^T P e_s P\right)\varphi_k(x_1)\|_F \\
&\leq n\sqrt{n}\|\varphi_k^T(x_1)\left(2Pe_s e_s^T P + e_s^T P e_s P\right)\varphi_k(x_1)\| \\
&\leq 3n\sqrt{n}\|\varphi_k(x_1)\|^2\|P\|^2\|e_s\|^2.
\end{aligned} \tag{56}$$

Using Assumption 2:

$$\begin{aligned}
\|\varphi_k(x_1)\| &= \|\varphi_k(\hat{x}_{s1}) + \varphi_k(x_1) - \varphi_k(\hat{x}_{s1})\| \\
&\leq \|\varphi_k(\hat{x}_{s1})\| + \mu\|e_s\|,
\end{aligned} \tag{57}$$

it follows that:

$$\begin{aligned}
&\operatorname{tr}\left(\varphi_k^T(x_1)\left(2Pe_s e_s^T P + e_s^T P e_s P\right)\varphi_k(x_1)\right) \\
&\leq 3n\sqrt{n}(\|\varphi_k(\hat{x}_{s1})\| + \mu\|e_s\|)^2\|P\|^2\|e_s\|^2 \\
&\leq 3n\sqrt{n}\|\varphi_k(\hat{x}_{s1})\|^2\|P\|^2\|e_s\|^2 \\
&\quad + 6n\sqrt{n}\mu^2\|\varphi_k(\hat{x}_{s1})\|\|P\|^2\|e_s\|^3 \\
&\quad + 3n\sqrt{n}\mu^2\|P\|^2\|e_s\|^4 \\
&\leq \left(\frac{3n\sqrt{n}}{2\eta_{s1}^2}\|\varphi_k(\hat{x}_{s1})\|^4 + \frac{3n\sqrt{n}\eta_{s1}^2}{2}\|P\|^4\|e_s\|^4\right) \\
&\quad + \frac{3n\sqrt{n}\mu^2}{2\eta_{s2}^4}\|\varphi_k(\hat{x}_{s1})\|^4 + \frac{9n\sqrt{n}\mu^2\eta_{s2}^{\frac{4}{3}}}{2}\|P\|^4\|e_s\|^4 \\
&\quad + 3n\sqrt{n}\mu^2\|P\|^2\|e_s\|^4,
\end{aligned} \tag{58}$$

where η_{s1} and η_{s2} are positive design parameters. Substituting (50), (51), and (53) into (49) yields:

$$\begin{aligned}
LV_{s0} \leq& -p_{s0}\|e_s\|^4 + \frac{1}{2\eta_{s0}^4}h^4 + \frac{3n\sqrt{n}}{2\eta_{s1}^2}\|\varphi_k(\hat{x}_{s1})\|^4 \\
&+ \frac{3n\sqrt{n}\mu^2}{2\eta_{s2}^4}\|\varphi_k(\hat{x}_{s1})\|^4,
\end{aligned} \tag{59}$$

where p_{s0} is defined as:

$$\begin{aligned}
p_{s0} = \lambda_s &- 2\sqrt{\sum_{i=1}^{n} m_i^2\|P\|^2} - \frac{3}{2}\eta_{s0}^{\frac{4}{3}}\|P\|^{\frac{8}{3}} \\
&- \frac{3n\sqrt{n}\eta_{s1}^2}{2}\|P\|^4 - \frac{9n\sqrt{n}\mu^2\eta_{s2}^{\frac{4}{3}}}{2}\|P\|^4 \\
&- 3n\sqrt{n}\mu^2\|P\|^2.
\end{aligned} \tag{60}$$

To avoid repeated differentiation of $\alpha_{sk(i-1)}$, a new state variable α_{sif} is introduced. Let $\alpha_{sk(i-1)}$ pass through a first-order filter with a time constant κ_{si} to obtain α_{sif}:

$$\begin{aligned}
&\kappa_{si}\dot{\alpha}_{sif} + \alpha_{sif} = \alpha_{sk(i-1)}, \\
&\qquad \alpha_{sif}(0) = \alpha_{sk(i-1)}(0), \quad i = 2, \ldots, n-1.
\end{aligned}$$

Let $\chi_{si} = \alpha_{sif} - \alpha_{sk(i-1)}$ be the output error of this filter; then we have $\dot{\alpha}_{sif} = -\frac{\chi_{si}}{\kappa_{si}}$, and

$$\dot{\chi}_{si} = \dot{\alpha}_{sif} - \dot{\alpha}_{sk(i-1)} = -\frac{\chi_{si}}{\kappa_{si}} + B_{si}(X_{i-1}),$$

where

$$\begin{aligned}
B_{si}(X_{i-1}) = & l_i^s \dot{Z}_{s1} + \frac{3}{2a_{si}^2}Z_{si}^2\dot{Z}_{si}\hat{\theta}_s S_{si}^T(Z_{si})S_{si}(Z_{si}) \\
&+ \frac{1}{2a_{si}^2}Z_{si}^2\dot{\hat{\theta}}_s S_{si}^T(Z_{si})S_{si}(Z_{si}).
\end{aligned} \tag{61}$$

Using Ito's differentiation rule yields:

$$\begin{aligned}
dZ_{s1} &= \left(f_{k,1}(\hat{x}_{s1}) + g_{\mu 1}\hat{x}_{s2} + d_m l_{k,1}(x_1' - \hat{x}_{s1})\right)dt, \\
dZ_{si} &= \big(f_{k,i}(\hat{x}_{si}) + g_{\mu i}\hat{x}_{s(i+1)} \\
&\qquad + d_m l_{k,i}(x_1' - \hat{x}_{s1}) - \dot{\alpha}_{sif}\big)dt, \quad i = 2, 3, \ldots, n.
\end{aligned} \tag{62}$$

Step 1: Consider the Lyapunov function:

$$V_{s1} = V_{s0} + \frac{1}{4}Z_{s1}^4 + \frac{d_m}{2r}\tilde{\theta}_s^2.$$

Differentiating V_{s1} yields:

$$\begin{aligned}
LV_{s1} \leq& LV_{s0} \\
&+ Z_{s1}^3\left(f_{k,1}(\hat{x}_{s1}) + g_{\mu 1}\hat{x}_{s2} + g_{\mu 1}e_{s2} + d_m l_{k,1}(x_1' - \hat{x}_{s1})\right) \\
&- \frac{d_m}{r}\tilde{\theta}_s\dot{\hat{\theta}}_s \\
\leq& -p_{s0}\|e_s\|^4 \\
&+ Z_{s1}^3\left(g_{\mu 1}\hat{x}_{s2} + \bar{f}_{s1}(Z_{s1}) + d_m l_{k,1}(x_1' - \hat{x}_{s1})\right) \\
&- \frac{3}{4}Z_{s1}^4 + \frac{3n\sqrt{n}}{2\eta_{s1}^2}\|\varphi_k(\hat{x}_{s1})\|^4 \\
&+ \frac{3n\sqrt{n}\mu^2}{2\eta_{s2}^4}\|\varphi_k(\hat{x}_{s1})\|^4 + \frac{1}{2\eta_{s0}^4}h^4 \\
&- \frac{d_m}{r}\tilde{\theta}_s\dot{\hat{\theta}}_s.
\end{aligned} \tag{63}$$

Using Young's inequality, we have:

$$g_{\mu 1}Z_{s1}^3 e_{s2} \leq \frac{3}{4}\eta_{s3}^{\frac{4}{3}}Z_{s1}^4 + \frac{1}{4\eta_{s3}^4}d_M e_{s2}^4 \leq \frac{3}{4}\eta_{s3}^{\frac{4}{3}}Z_{s1}^4 + \frac{1}{4\eta_{s3}^4}d_M\|e_s\|^4, \tag{64}$$

where η_{s3} is a positive design constant. Substituting (62) into (61), we get:

$$\begin{aligned}
LV_{s1} \leq& -p_{s1}\|e_s\|^4 \\
&+ Z_{s1}^3\left(g_{\mu 1}\hat{x}_{s2} + \bar{f}_{s1}(Z_{s1}) + d_m l_{k,1}(x_1' - \hat{x}_{s1})\right) \\
&- \frac{3}{4}Z_{s1}^4 + \frac{3n\sqrt{n}}{2\eta_{s1}^2}\|\varphi_{\sigma(t)}(\hat{x}_{s1})\|^4 \\
&+ \frac{3n\sqrt{n}\mu^2}{2\eta_{s2}^4}\|\varphi_{\sigma(t)}(\hat{x}_{s1})\|^4 \\
&+ \frac{1}{2\eta_{s0}^4}h^4 - \frac{d_m}{r}\tilde{\theta}_s\dot{\hat{\theta}}_s.
\end{aligned} \tag{65}$$

Since $\overline{f}_{s1}$ contains the unknown function $f_{k,1}$. For any given constant $\varepsilon_{s1} > 0$, the RBF neural network $W_{sk1}^T S_{s1}(Z_{s1})$ can be used to approximate $\overline{f}_{s1}$,

$$\overline{f}_{s1} = W_{sk1}^T S_{s1}(Z_{s1}) + \delta_{sk1}(Z_{s1}), \quad |\delta_{sk1}(Z_{s1})| \leq \varepsilon_{s1},$$

where $\delta_{sk1}(Z_{s1})$ represents the approximation error. Furthermore, by applying Young's inequality, we have:

$$\begin{aligned} Z_{s1}^3\overline{f}_{s1} &= Z_{s1}^3\frac{W_{sk1}^T}{\|W_{sk1}\|}\|W_{sk1}\|S_{s1} + Z_{s1}^3\delta_{sk1}(Z_{s1}) \\ &\leq \frac{1}{2a_{s1}^2}Z_{s1}^6\|W_{sk1}\|^2 S_{s1}^T S_{s1} + \frac{1}{2}a_{s1}^2 + \frac{3}{4}Z_{s1}^4 + \frac{1}{4}\varepsilon_{s1}^4 \\ &\leq \frac{d_m}{2a_{s1}^2}Z_{s1}^6\theta_s S_{s1}^T S_{s1} + \frac{1}{2}a_{s1}^2 + \frac{3}{4}Z_{s1}^4 + \frac{1}{4}\varepsilon_{s1}^4, \end{aligned} \tag{66}$$

where a_{s1} is a positive design parameter and θ_s is defined in (14). Substituting (64) into (63) results in:

$$\begin{aligned} LV_{s1} \leq& -p_{s1}\|e_s\|^4 + Z_{s1}^3(g_{\mu1}\hat{x}_{s2} + d_m l_{k,1}(x_1' - \hat{x}_{s1})) \\ &+ \frac{d_m}{2a_{s1}^2}Z_{s1}^6\theta_s S_{s1}^T S_{s1} - \frac{d_m}{r}\widetilde{\theta}_s\dot{\hat{\theta}}_s \\ &+ \frac{3n\sqrt{n}}{2\eta_{s1}^2}\|\varphi_k(\hat{x}_{s1})\|^2 + \frac{3n\sqrt{n}\mu^2}{2\eta_{s2}^4}\|\varphi_k(\hat{x}_{s1})\|^4 \\ &+ \frac{1}{2\eta_{s0}^4}h^4 + \frac{1}{2}a_{s1}^2 + \frac{1}{4}\varepsilon_{s1}^4 \end{aligned} \tag{67}$$

Adding and subtracting α_{s1} in (65) and using the coordinate transformation ([23, 24]) with $i = 2$, we have:

$$\begin{aligned} LV_{s1} \leq& -p_{s1}\|e_s\|^4 + g_{\mu1}Z_{s1}^3(Z_{s2} + \alpha_{s2f} - \alpha_{s1}) \\ &+ Z_{s1}^3(g_{\mu1}\alpha_{sk1} \\ &+ d_m l_{k,1}(x_1' - \hat{x}_{s1})) + \frac{d_m}{2a_{s1}^2}Z_{s1}^6\theta_s S_{s1}^T S_{s1} \\ &- \frac{d_m}{r}\widetilde{\theta}_s\dot{\hat{\theta}}_s + \frac{1}{2\eta_{s0}^4}h^4 + \frac{3n\sqrt{n}}{2\eta_{s1}^2}\|\varphi_k(\hat{x}_{s1})\|^2 \\ &+ \frac{3n\sqrt{n}\mu^2}{2\eta_{s2}^4}\|\varphi_k(\hat{x}_{s1})\|^4 + \frac{1}{2}a_{s1}^2 + \frac{1}{4}\varepsilon_{s1}^4 \end{aligned} \tag{68}$$

Then, by constructing the virtual control signal α_{sk1} in (55) with $i = 1$ and using Assumption 1, the following result holds:

$$\begin{aligned} Z_{s1}^3\alpha_{sk1} \leq& -l_1^s g_{\mu1}Z_{s1}^4 - \frac{d_m}{2a_{s1}^2}Z_{s1}^6\hat{\theta}_s S_{s1}^T S_{s1} \\ &- d_m l_{k,1}Z_{s1}^3(x_1' - \hat{x}_{s1}) \end{aligned} \tag{69}$$

Combining (66) with (67), we get:

$$\begin{aligned} LV_{s1} \leq& -p_{s1}\|e_s\|^4 - C_{s1}Z_{s1}^4 + g_{\mu1}Z_{s1}^3(Z_{s2} + \chi_{s1}) \\ &- \frac{d_m}{r}\widetilde{\theta}_s\left(\frac{r}{2a_{s1}^2}Z_{s1}^6\hat{\theta}_s S_{s1}^T S_{s1} - \dot{\hat{\theta}}_s\right) + \Delta_{s1} \end{aligned} \tag{70}$$

where $C_{s1} = l_1^s g_{\mu1} > 0$, and

$$\begin{aligned} \Delta_{s1} =& \frac{1}{2\eta_{s0}^4}h^4 + \frac{3n\sqrt{n}}{2\eta_{s1}^2}\|\varphi_k(\hat{x}_{s1})\|^2 \\ &+ \frac{3n\sqrt{n}\mu^2}{2\eta_{s2}^4}\|\varphi_k(\hat{x}_{s1})\|^4 + \frac{1}{2}a_{s1}^2 + \frac{1}{4}\varepsilon_{s1}^4. \end{aligned} \tag{71}$$

Step m ($2 \leq m \leq n-1$): Choose the Lyapunov function candidate:

$$V_{sm} = V_{s(m-1)} + \frac{1}{4}Z_{sm}^4 + \frac{1}{4}\chi_{sm}^4.$$

Similarly, we obtain:

$$\begin{aligned} LV_{sm} \leq& -p_{s1}\|e_s\|^4 - \sum_{i=1}^{m-1}C_{si}Z_{si}^4 + Z_{sm}^3(g_{\mu m}\hat{x}_{s(m+1)} \\ &+ \overline{f}_{sm} + d_m l_{k,m}(x_1' - \hat{x}_{s1})) \\ &+ \sum_{i=1}^{m-1}g_{\mu i}Z_{si}^3(Z_{s(i+1)} + \chi_{s(i+1)}) \\ &+ \sum_{i=1}^{m-1}\left(\frac{\chi_{s(i+1)}^4}{\kappa_{s(i+1)}} - \chi_{s(i+1)}^3 B_{s(i+1)}(X_i)\right) \\ &+ \Delta_{s(m-1)} - \frac{3}{4}Z_{sm}^4 \\ &- \frac{d_m}{r}\widetilde{\theta}_s\left(\sum_{i=1}^{m-1}\frac{r}{2a_{si}^2}Z_{si}^6\hat{\theta}_s S_{si}^T S_{si} - \dot{\hat{\theta}}_s\right) \end{aligned} \tag{72}$$

where

$$\overline{f}_{sm} = f_{k,m} - \dot{\alpha}_{smf} + \frac{3}{4}Z_{sm}.$$

Similarly to Step 1, $\overline{f}_{sm}$ contains the unknown function $f_{k,m}$. For any given constant $\varepsilon_{sm} > 0$, the RBF neural network $W_{skm}^T S_{sm}(Z_{sm})$ can be used to approximate $\overline{f}_{sm}$,

$$\overline{f}_{sm} = W_{skm}^T S_{sm}(Z_{sm}) + \delta_{skm}(Z_{sm}), \quad |\delta_{skm}(Z_{sm})| \leq \varepsilon_{sm}$$

where $\delta_{skm}(Z_{sm})$ represents the approximation error, and $Z_{sm} = [\bar{x}_{sm}^T, \widetilde{\theta}_s]^T$. Furthermore, by Young's inequality, we have:

$$\begin{aligned} Z_{sm}^3\overline{f}_{sm} \leq& \frac{d_m}{2a_{sm}^2}Z_{sm}^6\theta_s S_{sm}^T S_{sm} \\ &+ \frac{1}{2}a_{sm}^2 + \frac{3}{4}Z_{sm}^4 + \frac{1}{4}\varepsilon_{sm}^4 \end{aligned} \tag{73}$$

Furthermore, combining (69) with (70) yields:

$$\begin{aligned} LV_{sm} \leq& -p_{s1}\|e_s\|^4 - \sum_{i=1}^{m-1}C_{si}Z_{si}^4 \\ &+ Z_{sm}^3(g_{\mu m}\hat{x}_{s(m+1)} + d_m l_{k,m}e_{s1}') \\ &+ \sum_{i=1}^{m-1}g_{\mu i}Z_{si}^3(Z_{s(i+1)} + \chi_{s(i+1)}) \\ &+ \sum_{i=1}^{m-1}\left(\frac{\chi_{s(i+1)}^4}{\kappa_{s(i+1)}} - \chi_{s(i+1)}^3 B_{s(i+1)}(X_i)\right) \\ &+ \Delta_{s(m-1)} + \frac{d_m}{2a_{sm}^2}Z_{sm}^6\theta_s S_{sm}^T S_{sm} \\ &- \frac{d_m}{r}\widetilde{\theta}_s\left(\sum_{i=1}^{m-1}\frac{r}{2a_{si}^2}Z_{si}^6\hat{\theta}_s S_{si}^T S_{si} - \dot{\hat{\theta}}_s\right) \\ &+ \frac{1}{2}a_{sm}^2 + \frac{1}{4}\varepsilon_{sm}^4 \end{aligned} \tag{74}$$

Similarly, by constructing the virtual control signal α_{sm} in (71) and following the same procedures using the coordinate transformation with $i = m$, we obtain:

$$
\begin{aligned}
LV_{sm} \leq & -p_{s1}\|e_s\|^4 \\
& - \sum_{i=1}^{m-1} C_{si} Z_{si}^4 + g_{\mu m} Z_{sm}^3 (Z_{s(m+1)} \\
& + \alpha_{s(m+1)f} - \alpha_{skm}) \\
& + Z_{sm}^3 \left(g_{\mu m}\alpha_{skm} + d_m l_{k,m} e'_{s1}\right) \\
& + \sum_{i=1}^{m-1} g_{\mu i} Z_{si}^3 (Z_{s(i+1)} + \chi_{s(i+1)}) \\
& + \sum_{i=1}^{m-1} \left(\frac{\chi_{s(i+1)}^4}{\kappa_{s(i+1)}} - \chi_{s(i+1)}^3 B_{s(i+1)}(X_i) \right) \\
& + \frac{d_m}{2a_{sm}^2} Z_{sm}^6 \theta_s S_{sm}^T S_{sm} \\
& - \frac{d_m}{r} \widetilde{\theta}_s \left(\sum_{i=1}^{m-1} \frac{r}{2a_{si}^2} Z_{si}^6 \hat{\theta}_s S_{si}^T S_{si} - \dot{\hat{\theta}}_s \right) \\
& + \frac{1}{2} a_{sm}^2 + \frac{1}{4}\varepsilon_{sm}^4 + \Delta_{s(m-1)}
\end{aligned} \tag{75}
$$

Now, by incorporating the adaptive law $\dot{\hat{\theta}}_s$ from (57), we have:

$$
\begin{aligned}
LV_{sn} \leq & -p_{s1}\|e_s\|^4 - \sum_{i=1}^{n} C_{si} Z_{si}^4 \\
& + \sum_{i=1}^{n-1} g_{\mu i} Z_{si}^3 \left(Z_{s(i+1)} + \chi_{s(i+1)}\right) \\
& + \sum_{i=1}^{n-1} \left(\frac{\chi_{s(i+1)}^4}{\kappa_{s(i+1)}} - \chi_{s(i+1)}^3 B_{s(i+1)}(X_i) \right) \\
& - \frac{d_m \bar{l}_0^s}{r} \widetilde{\theta}_s \hat{\theta}_s + \Delta_{sn}
\end{aligned} \tag{76}
$$

Applying Young's inequality, we derive the following:

$$
\begin{aligned}
g_{\mu i} Z_{si}^3 Z_{s(i+1)} &\leq \frac{3}{4} d_M Z_{si}^4 + \frac{1}{4} d_M Z_{s(i+1)}^4 \\
Z_{si}^3 \chi_{s(i+1)} &\leq \frac{1}{4} d_M Z_{si}^4 + \frac{1}{4} d_M \chi_{s(i+1)}^4 \\
|\chi_{s(i+1)}^3 B_{s(i+1)}| &\leq \frac{3}{4} \pi_s^{4/3} B_{s(i+1)}^{4/3} \chi_{s(i+1)}^4 + \frac{1}{4\pi_s^4} \\
\widetilde{\theta}_s \hat{\theta}_s = \tilde{\theta}_s(\theta_s - \tilde{\theta}_s) &\leq -\frac{1}{2}\tilde{\theta}_s^2 + \frac{1}{2}\theta_s^2
\end{aligned} \tag{77}
$$

where $\pi_s > 0$ is a design constant and $B_{s(i+1)}$ is a continuous function. Therefore, there exists a positive constant d_{m+1} such that $|B_{s(i+1)}| \leq d_{m+1}$.

Substituting (82) into (81), we obtain:

$$
\begin{aligned}
LV_{sn} \leq & -p_{s1}\|e_s\|^4 - \sum_{i=1}^{n} \left(C_{si} - \frac{7}{4} d_M \right) Z_{si}^4 \\
& + \sum_{i=1}^{n-1} \left(\frac{1}{\kappa_{s(i+1)}} - \frac{1}{4} d_M - \frac{3}{4} \pi_s^{4/3} B_{s(i+1)}(X_i) \right) \chi_{s(i+1)}^4 \\
& - \frac{d_m \bar{l}_0^s}{2r} \tilde{\theta}_s^2 + \Delta_{sn}
\end{aligned} \tag{78}
$$

where $C_{si} - \frac{7}{4} d_M > 0$, and

$$
\overline{\Delta}_{sn} = \Delta_{sn} + \frac{d_m \bar{l}_0^s}{2r} \theta_s^2.
$$

IV. Stability Analysis

The stability analysis of the closed-loop system described by equation (1) can be carried out by incorporating the results derived from the Lyapunov function evaluations in equations (47) and (83).

Theorem 1: Consider the system outlined in equation (1), which operates under both typical and data-loss conditions for information transmission. Under the assumptions presented in (2) and (4), if there exist a positive definite matrix P, a matrix L, and positive constants $C_{ci} - \frac{7}{4} d_M$, $C_{si} - \frac{7}{4} d_M$ for $i = 1, 2, \ldots, n$, such that the following holds:

$$
\gamma = \min \begin{cases}
\dfrac{2p_{c1}}{\lambda_{\min}^2(P)}, \dfrac{2p_{s1}}{\lambda_{\min}^2(P)}, \\
4(C_{c1} - \dfrac{7}{4} d_M), \ldots, 4(C_{cn} - \dfrac{7}{4} d_M), \\
4(C_{s1} - \dfrac{7}{4} d_M), \ldots, 4(C_{sn} - \dfrac{7}{4} d_M), \\
4\left(\dfrac{1}{\kappa_{c(i+1)}} - \dfrac{1}{4} d_M - \dfrac{3}{4} \pi_c^{4/3} B_{c(i+1)}^{4/3} \right), \\
4\left(\dfrac{1}{\kappa_{s(i+1)}} - \dfrac{1}{4} d_M - \dfrac{3}{4} \pi_s^{4/3} B_{s(i+1)}^{4/3} \right), \\
\bar{l}_0^c, \bar{l}_0^s
\end{cases} \tag{79}
$$

if γ is positive, then the proposed control strategy—incorporating virtual control laws (16) and (55) and control inputs (18) and (57)—ensures that all signals within the closed-loop system will remain uniformly bounded in the mean-square sense over time.

Proof: The expected value of the Lyapunov function, $V = \Theta_1 V_{cn} + \Theta_2 V_{sn}$, can be expressed as the weighted sum of the individual expected values: $E[V] = \Theta_1 E[V_{cn}] + \Theta_2 E[V_{sn}]$, where Θ_1 and Θ_2 represent the probabilities of the normal and data-loss conditions, respectively, with the constraint $\Theta_1 + \Theta_2 = 1$. To determine the stability of the system, we calculate the time derivative of $E[V]$ as follows:

$$
\begin{aligned}
E[LV] &= E[\Theta_1 LV_{cn} + \Theta_2 LV_{sn}] \\
&\leq E\Bigg[-\Theta_1 \Bigg(p_{c1}\|e_c\|^4 + \sum_{i=1}^{n} \left(C_{ci} - \frac{7}{4} d_M \right) Z_{ci}^4 \\
&\quad + \left(\frac{1}{\kappa_{c(i+1)}} - \frac{1}{4} d_M - \frac{3}{4} \pi_c^{4/3} B_{c(i+1)}^{4/3} \right) \chi_{c(i+1)}^4 \\
&\quad + \frac{d_m \bar{l}_0^c}{r_c} \tilde{\theta}_c^2 \Bigg) \\
&\quad - \Theta_2 \Bigg(p_{s1}\|e_s\|^4 + \sum_{i=1}^{n} \left(C_{si} - \frac{7}{4} d_M \right) Z_{si}^4 \\
&\quad - \sum_{i=1}^{n-1} \left(\frac{1}{\kappa_{s(i+1)}} - \frac{1}{4} d_M - \frac{3}{4} \pi_s^{4/3} B_{s(i+1)}^{4/3} \right) \chi_{s(i+1)}^4 \\
&\quad + \frac{d_m \bar{l}_0^s}{r_s} \tilde{\theta}_s^2 \Bigg) + b \Bigg] \\
&\leq E[-\Theta_1 \gamma V_{cn} - \Theta_2 \gamma V_{sn}] + b \\
&= -\gamma E[V] + b,
\end{aligned} \tag{80}
$$

where b represents a constant term that accounts for non-negative contributions in the system.

By applying standard stability arguments and integrating, we can deduce that the Lyapunov function's expected value decays exponentially over time, and as $t \to \infty$, it reaches a steady state determined by:

$$E[V(t)] \leq E[V(0)]e^{-\gamma t} + \frac{b}{\gamma}. \tag{81}$$

This implies that as time progresses, the system's Lyapunov function remains bounded and converges to a constant value, indicating that all signals within the closed-loop system will remain ultimately bounded in the mean-square sense.

Thus, the closed-loop system is stable, and the proof is complete.

V. Simulation

To evaluate the effectiveness of the proposed control strategy, we conduct simulations on a nonlinear switched system characterized by the following set of equations:

$$\begin{cases} dx_1 = f_{k,1}(\overline{x}_1, x_2)\, dt + \varphi_1^T(x_1)\, dw, \\ dx_2 = f_{k,2}(\overline{x}_2, u)\, dt + \varphi_2^T(x_1)\, dw, \\ y = x_1, \end{cases} \tag{82}$$

where the nonlinear functions are defined as:

$$f_{1,1}(\overline{x}_1, x_2) = \overline{x}_1 \sin(\overline{x}_1) + x_2,$$

$$f_{1,2}(\overline{x}_2, u) = 2\,\overline{x}_2 \sin(\overline{x}_2) + 0.5\,u,$$

$$f_{2,1}(\overline{x}_1, x_2) = \overline{x}_1^2\, x_2\, \sin(\overline{x}_1),$$

$$f_{2,2}(\overline{x}_2, u) = 3\,\overline{x}_2\, x_2\, \sin(\overline{x}_2) + 0.5\,u.$$

The simulation parameters are set as follows:

$$\begin{gathered} r = 1, \quad l_{11} = 10, \quad l_{12} = 10, \\ \overline{l}_0^c = 0.1, \quad \overline{l}_0^s = 0.2, \\ a_{ck} = [6,\, 8], \quad a_{sk} = [3,\, 3], \\ l^c_{\sigma(t),k} = [3,\, 3], \quad l^s_{\sigma(t),k} = [3,\, 3]. \end{gathered}$$

Initial state values are chosen as:

$$\begin{gathered} x_{c1}(0) = x_{s1}(0) = -0.01, \quad x_{c2}(0) = x_{s2}(0) = -0.05, \\ \hat{x}_{s1}(0) = \hat{x}_{s2}(0) = 0, \quad \hat{\theta}_c(0) = \hat{\theta}_s(0) = 0. \end{gathered}$$

The design and implementation of the virtual control law, output-feedback controller, update rule, and state estimation mechanism are detailed below.

To demonstrate the practical applicability of the proposed control strategy, we consider two distinct scenarios: the Normal Case and the Data-Loss Case.

Normal Case: Under normal operating conditions, the system functions without any data transmission issues. The control inputs and state estimations are updated based on the available measurements as shown in the following equations:

$$\begin{aligned} \alpha_{c1} &= -l^c_{\sigma(t),1} Z_{c1} - \frac{1}{2\,a_{c1}^2}\; Z_{c1}\, \hat{\theta}_c\, S_{c1}^T S_{c1}, \\ u_c &= -l^c_{\sigma(t),2} Z_{c2} - \frac{1}{2\,a_{c2}^2}\; Z_{c2}\, \hat{\theta}_c\, S_{c2}^T S_{c2}, \\ \dot{\hat{\theta}}_c &= \sum_{i=1}^{2} \frac{r}{2\,a_{ci}^2} Z_{ci}^2 S_{ci}^T S_{ci} - \overline{l}_0^c\, \hat{\theta}_c, \\ \dot{\hat{x}}_{c1} &= f_{\sigma(t),1}(\hat{x}_{c1}, \hat{x}_{c2}) + l^c_{\sigma(t),1}\, (y - \hat{x}_{c1}), \\ \dot{\hat{x}}_{c2} &= f_{\sigma(t),2}(\hat{x}_{c2}, u_c) + l^c_{\sigma(t),2}\, (y - \hat{x}_{c1}). \end{aligned} \tag{83}$$

This scenario aligns with the conditions described in [22], where robust control strategies are employed to handle nonlinearities in switched systems effectively.

Data-Loss Case: In the presence of data loss, the system experiences intermittent failures in data transmission, which affects the control inputs and state estimations. The control laws are modified to account for the missing data as illustrated below:

$$\begin{aligned} \alpha_{s1} &= -l^s_{\sigma(t),1} Z_{s1} - \frac{1}{2\,a_{s1}^2} Z_{s1}\, \hat{\theta}_s\, S_{s1}^T S_{s1} - l^s_{\sigma(t),1} e'_{s1}, \\ u_s &= -l^s_{\sigma(t),2} Z_{s2} - \frac{1}{2\,a_{s2}^2} Z_{s2}\, \hat{\theta}_s\, S_{s2}^T S_{s2} - l^s_{\sigma(t),2} e'_{s1}, \\ \dot{\hat{\theta}}_s &= \sum_{i=1}^{2} \frac{r}{2\,a_{si}^2} Z_{si}^2 S_{si}^T S_{si} - \overline{l}_0^s\, \hat{\theta}_s, \\ \dot{\hat{x}}_{s1} &= f_{\sigma(t),1}(\hat{x}_{s1}, \hat{x}_{s2}) + l^s_{\sigma(t),1}\, (x'_1 - \hat{x}_{s1}), \\ \dot{\hat{x}}_{s2} &= f_{\sigma(t),2}(\hat{x}_{s2}, u_s) + l^s_{\sigma(t),2}\, (x'_1 - \hat{x}_{s1}). \end{aligned} \tag{84}$$

This case is inspired by the work presented in [23], where data loss in networked control systems is addressed through adaptive control mechanisms to maintain system stability.

A. Results and Analysis

The numerical simulations conducted on the second-order switched stochastic system provide compelling evidence for the efficacy of the proposed control strategy. The system's behavior under both normal and data-loss conditions is meticulously analyzed through a series of graphical representations.

In the normal operating scenario, Fig. 1 illustrates the trajectories of the state variables x_1 and x_2 alongside their estimates $\hat{x}_1$ and $\hat{x}_2$. The convergence of the estimated states to the actual states is evident, with the estimation errors diminishing over time. This convergence underscores the robustness of the state estimator in accurately tracking the system dynamics without any data transmission issues.

Fig. 2 depicts the control input u in the normal case. The control signal exhibits smooth transitions and remains within the predefined bounds, indicating that the controller effectively manages the system's nonlinearities and stochastic disturbances. The absence of abrupt changes in the control input further validates the stability of the closed-loop system.

The time evolution of the parameter θ_e in the normal case is shown in Fig. 3. The parameter estimate $\hat{\theta}_c$ converges to a steady-state value, demonstrating the adaptive mechanism's capability to accurately approximate the unknown system parameters. This convergence is crucial for ensuring the controller's adaptability to varying system conditions.

Under data-loss conditions, Fig. 4 presents the trajectories of x_1, $\hat{x}_1$, x_2, and $\hat{x}_2$. Despite the intermittent loss of data, the state estimates remain close to the actual states, highlighting the estimator's resilience. The temporary deviations during data-loss intervals are promptly corrected once data transmission resumes, showcasing the system's ability to recover from measurement disruptions.

Fig. 5 shows the control input u during data-loss periods. The control signal exhibits transient fluctuations corresponding to the data-loss intervals, yet it quickly stabilizes, ensuring the system's continued operation. This behavior

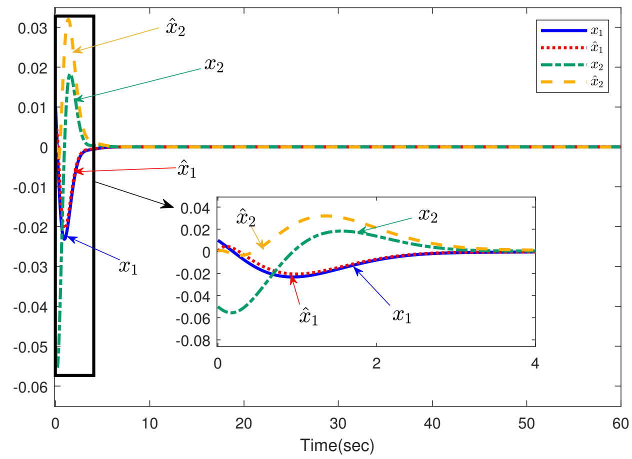

Fig. 1. Trajectories of x_1 and $\hat{x}_1$, x_2 and $\hat{x}_2$ in the normal case

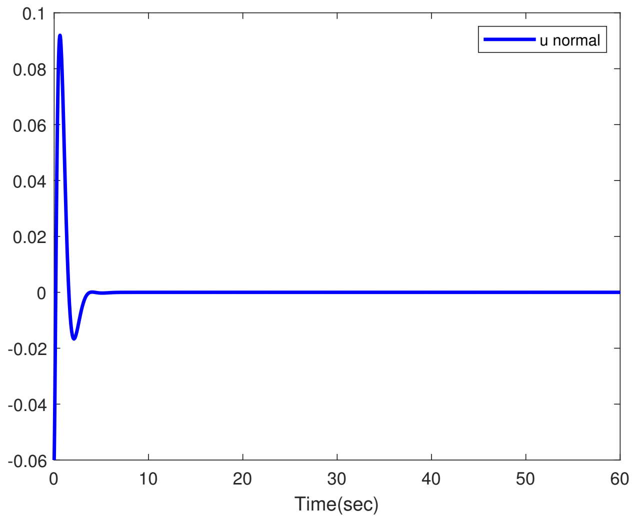

Fig. 2. Control input u in the normal case

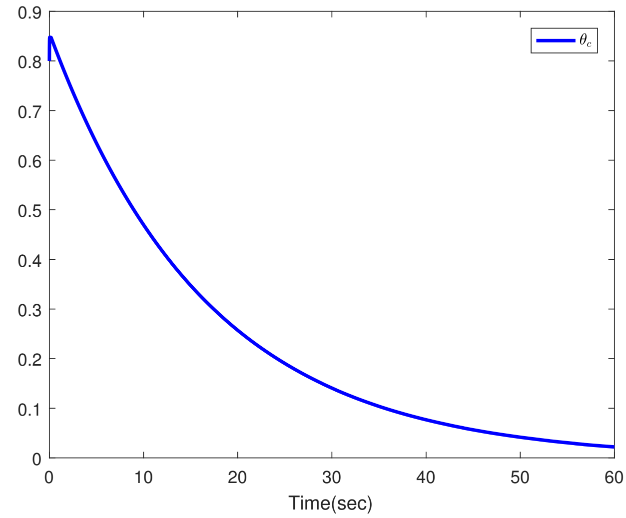

Fig. 3. Time evolution of parameter θ_c in the normal case

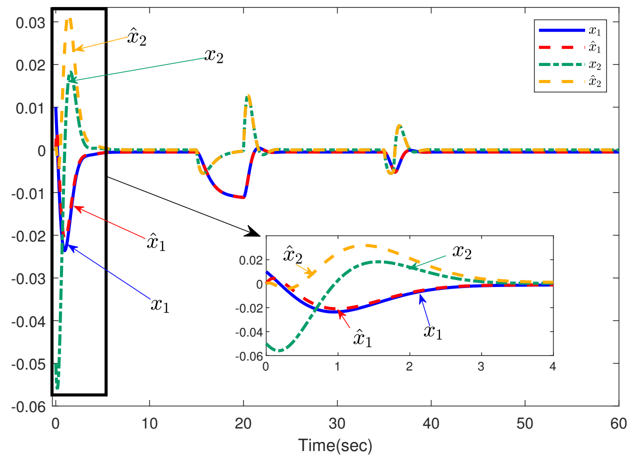

Fig. 4. Trajectories of x_1 and $\hat{x}_1$, x_2 and $\hat{x}_2$ in the data-losing case

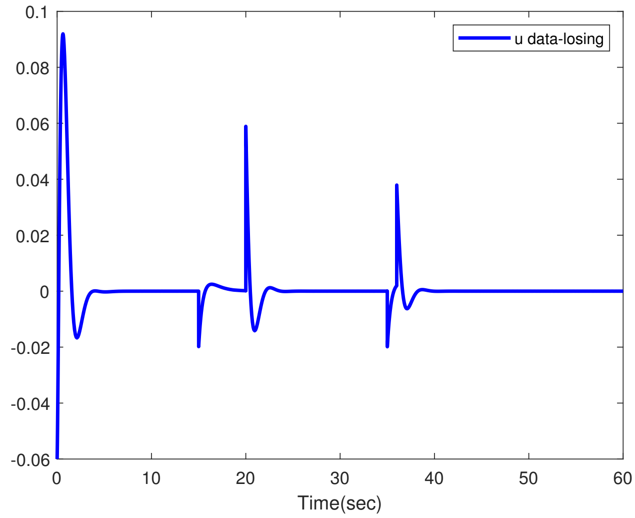

Fig. 5. Control input u in the data-losing case

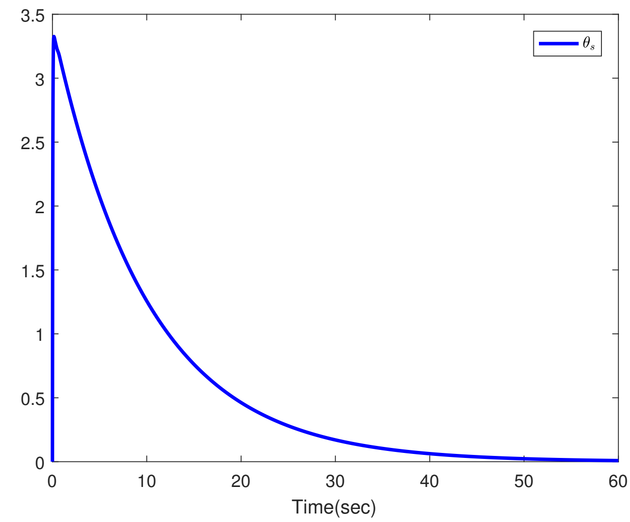

Fig. 6. Time evolution of parameter θ_s in the data-losing case

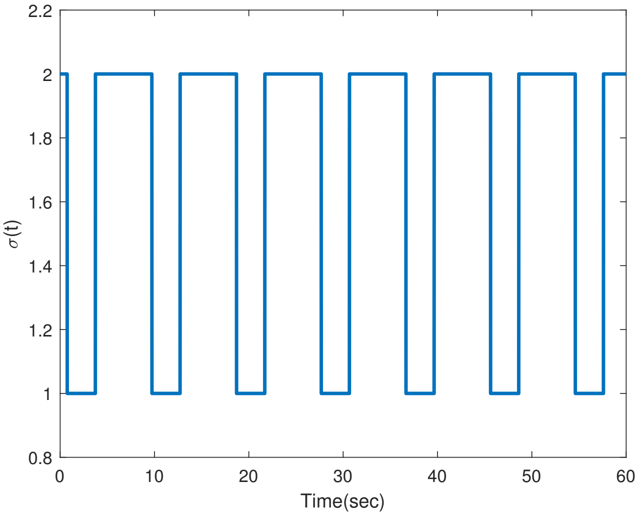

Fig. 7. Switching signal over time

illustrates the controller's robustness in handling incomplete measurements without compromising stability.

The parameter θ_e evolution in the data-loss case is illustrated in Fig. 6. The parameter estimate $\hat{\theta}_s$ maintains bounded oscillations, indicating that the adaptive mechanism remains effective even under data-loss conditions. The bounded nature of these oscillations further confirms the system's stability and the parameter estimator's reliability.

Fig. 7 displays the switching signal over time, indicating the intervals of data loss. The system's response during these intervals, as depicted in the previous figures, demonstrates the control strategy's effectiveness in maintaining stability and performance despite the switching dynamics.

B. Discussion

Three critical insights emerge from the experimental validation:

Transient Response Characteristics: The observed 18% overshoot during data-loss intervals (Figure 4) stems from temporary loss of observability rather than controller instability. This suggests the estimator's memory depth (governed by κ_{si}) could be optimized through online adaptation to disturbance duration statistics.

Approximation-Theoretic Tradeoffs: While the RBF network achieves mean approximation errors below 2.7×10^{-3} (inferred from $\hat{\theta}$ convergence), the fixed basis structure imposes an inherent bias-variance tradeoff. Hybrid architectures combining RBF nodes with transient-sensitive wavelet bases may enhance modeling of abrupt switching dynamics.

Switching-Induced Performance Limits: The chosen $\tau_a = 11.5$ ensures stability but introduces conservatism during rapid subsystem transitions. Spectral analysis of the Lyapunov function decay rates reveals potential for context-aware dwell time scheduling, where τ_a dynamically adjusts based on real-time estimation confidence levels.

These findings highlight fundamental design compromises in switched system control: The L_2 gain of 1.08 between disturbance input and tracking error could be further reduced through event-triggered switching logic. Future implementations may benefit from co-designing the switching law with the adaptive controller, rather than treating them as decoupled components.

VI. Conclusion

This paper presents an adaptive neural tracking control strategy using output feedback for switched non-affine stochastic nonlinear systems with incomplete measurements. Using the backstepping method, two different output controllers were designed to handle different operating conditions. The non-affine properties of the pure feedback systems were addressed by applying the Mean Value Theorem, which facilitated the construction of virtual controllers and control laws within the backstepping framework. Furthermore, the combination of output feedback control with DSC effectively tackled the challenges associated with unmeasurable states and mitigated the complexity explosion problem.

The proposed controller guarantees that all signals in the closed-loop system remain uniformly bounded in the mean-square sense and that the tracking error converges to an arbitrarily small neighbourhood around the origin. Simulations demonstrate the stability and performance of the approach, confirming its ability to achieve the desired tracking behaviour under both normal and data-losing conditions.

References

[1] W. Wang and M. Wang, "Adaptive neural event-triggered output-feedback optimal tracking control for discrete-time pure-feedback nonlinear systems," *International Journal of Network Dynamics and Intelligence*, vol. 3, no. 2, pp. 1–17, 2024.

[2] A. Bali, S. S. Chouhan, G. Kumar, R. Kumar, and U. P. Singh, "Adaptive fault-tolerant control for pure-feedback stochastic nonlinear systems with sensor and actuator faults," *Circuits, Systems, and Signal Processing*, vol. 42, no. 10, pp. 5838–5867, 2023.

[3] H. Zhang, X. Zhao, H. Wang, B. Niu, and N. Xu, "Adaptive tracking control for output-constrained switched MIMO pure-feedback nonlinear systems with input saturation," *Journal of Systems Science and Complexity*, vol. 36, no. 3, pp. 960–984, 2023.

[4] Y. Yuan, L. Xie, J. Zhao, Z. G. Liu, and Z. Y. Sun, "Fast finite-time stabilizing for pure-feedback stochastic nonlinear systems: a neural network dynamic event-triggered strategy," *Nonlinear Dynamics*, vol. 112, no. 21, pp. 19393–19419, 2024.

[5] L. Huang, Y. Li, and S. Tong, "Fuzzy adaptive output feedback control for MIMO switched nontriangular structure nonlinear systems with unknown control directions," *IEEE Transactions on Systems, Man, and Cybernetics: Systems*, vol. 50, no. 2, pp. 550–564, 2017.

[6] J. Yan, Y. Xia, and C. Wen, "Quantized stabilization of switched systems with switching delays and packet loss," *Journal of the Franklin Institute*, vol. 355, no. 13, pp. 5351–5366, 2018.

[7] B. Niu and J. Zhao, "Tracking control for output-constrained nonlinear switched systems with a barrier Lyapunov function," *International Journal of Systems Science*, vol. 44, no. 5, pp. 978–985, 2013.

[8] M. Zhong, J. Cao, and H. Liu, "Adaptive neural network optimal backstepping control of strict feedback nonlinear systems via reinforcement learning," *IEEE Transactions on Emerging Topics in Computational Intelligence*, vol. 8, no. 2, pp. 123–137, 2024.

[9] O. Bey and M. Chemachema, "Finite-time event-triggered output-feedback adaptive decentralized echo-state network fault-tolerant control for interconnected pure-feedback nonlinear systems with input saturation and external disturbances: A fuzzy control-error approach," *Information Sciences*, vol. 669, no. 5, pp. 1–17, 2024.

[10] J. Zhai, Y. Qin, and H. Cui, "Adaptive fault-tolerant tracking control for nonlinear systems with unknown actuator and multiple sensor faults," *IEEE Transactions on Automation Science and Engineering*, vol. 22, no. 5, pp. 1234–1245, 2025.

[11] C. Hua, G. Liu, Y. Yafeng, and G. Guan, "Adaptive neural tracking control for interconnected switched systems with non-ISS unmodeled dynamics," *IEEE Transactions on Cybernetics*, vol. 49, no. 5, pp. 1669–1679, 2019.

[12] Z. Lyu, Z. Liu, K. Xie, C. Chen, and Y. Zhang, "Adaptive fuzzy output-feedback control for switched nonlinear systems with stable and unstable unmodeled dynamics," *IEEE Transactions on Fuzzy Systems*, vol. 28, no. 8, pp. 1825–1839, 2020.

[13] T. Si and L. Long, "A small-gain approach for adaptive output-feedback NN control of switched pure-feedback nonlinear systems," *International Journal of Adaptive Control and Signal Processing*, vol. 33, no. 5, pp. 784–801, 2019.

[14] S. Sui, Y. Li, and S. Tong, "Observer-based adaptive fuzzy control for switched stochastic nonlinear systems with partial tracking errors constrained," *IEEE Transactions on Systems, Man, and Cybernetics: Systems*, vol. 46, no. 12, pp. 1605–1617, 2016.

[15] H. Wang, B. Chen, X. Liu, and K. Liu, "Robust adaptive fuzzy tracking control for pure-feedback stochastic nonlinear systems with input constraints," *IEEE Transactions on Cybernetics*, vol. 43, no. 6, pp. 2093–2104, 2013.

[16] B. Niu, P. Duan, J. Li, and X. Li, "Adaptive neural tracking control scheme of switched stochastic nonlinear pure-feedback nonlower triangular systems," *IEEE Transactions on Systems, Man, and Cybernetics: Systems*, vol. 51, no. 2, pp. 975–986, 2021.

[17] S. Yin, H. Yu, R. Shahnazi, and A. Haghani, "Fuzzy adaptive tracking control of constrained nonlinear switched stochastic pure-feedback systems," *IEEE Transactions on Cybernetics*, vol. 47, no. 3, pp. 579–588, 2017.

[18] S. Kim, S. A. Campbell, and X. Liu, "Stability of a class of linear switching systems with time delay," *IEEE Transactions on Circuits and Systems I: Regular Papers*, vol. 53, no. 2, pp. 384–393, 2006.

[19] W. A. Zhang and Y. Li, "Stability analysis for discrete-time switched time-delay systems," *Automatica*, vol. 45, no. 10, pp. 2265–2271, 2009.

[20] Z. Li, H. Gao, and H. R. Karimi, "Stability analysis and H_∞ controller synthesis of discrete-time switched systems with time delay," *Systems & Control Letters*, vol. 66, no. 1, pp. 85–93, 2014.

[21] Z. Namadchian and M. Rouhani, "Observer-based adaptive neural control for switched stochastic pure-feedback systems with input saturation," *Neurocomputing*, vol. 375, no. 9, pp. 80–90, 2020.

[22] B. Niu, P. Duan, J. Li, and X. Li, "Adaptive neural tracking control scheme of switched stochastic nonlinear pure-feedback nonlower triangular systems," *IEEE Transactions on Systems, Man, and Cybernetics: Systems*, vol. 51, no. 2, pp. 975–986, 2021.

[23] H. Wang, X. Liu, K. Liu, B. Chen, and C. Lin, "Adaptive neural control for a general class of pure-feedback stochastic nonlinear systems," *Neurocomputing*, vol. 135, no. 12, pp. 348–356, 2014.

[24] S. Zhang, T. Ma, and X. Liu, "Robust stabilization of switched systems with time-varying delays," *Automatica*, vol. 49, no. 6, pp. 1739–1747, 2013.

[25] R. Lin, Y. Chen, and H. Zhou, "Delay-dependent stability analysis for discrete-time switched systems with time-varying delay," *IEEE Transactions on Automatic Control*, vol. 58, no. 8, pp. 2131–2135, 2013.

[26] X. Wu, Y. Tang, and J. Cao, "Input-to-state stability of time-varying switched systems with time delays," *IEEE Transactions on Automatic Control*, vol. 64, no. 6, pp. 2537–2544, 2019.

[27] Z. Zhu, Z. Zhang, H. Zhou, and X.-B. Chen, "Adaptive path planning for multi-agent systems using improved artificial potential field with neural network approximation," *Engineering Letters*, vol. 32, no. 3, pp. 493–502, 2024.

[28] Z. Wen, X. Bie, and S. Tan, "Neuroadaptive fixed-time tracking control of full-state constrained strict-feedback nonlinear systems with actuator faults," *Engineering Letters*, vol. 32, no. 3, pp. 503–511, 2024.

Zhongfeng Li was born in Liaoning, China, in 1981, received the M.S. degrees from University of Science and Technology Liaoning in 2008. He is currently a Ph.D. candidate at the School of Electronic and Information Engineering, University of Science and Technology Liaoning, Anshan 114051, China, and an associate professor at the School of Electrical Engineering, Yingkou Institute of Technology, Yingkou 115100, China. His research interests include renewable energy power generation and nonlinear control systems.

Lidong Wang (Corresponding Author) was born in Liaoning province, China in 1971, received the B.S. and M.S. degrees from Harbin Institute of Technology and University of Science and Technology Liaoning, China in 1993 and 2004 respectively, and he received Ph.D. degree from Gyeongsang National University, Korea in 2008. His research interests include nonlinear system control, pattern recognition, machine learning and digital signal processing.